A Thesis

Entitled

A Novel Device for Delivering Combined Partial Breast Irradiation and Partial Breast Hyperthermia

By

Todd A. White

Submitted to the Graduate Faculty as partial fulfillment of the requirements for the Master of Science in Biomedical Science Degree in Medical Physics

_____

Dr. E. Ishmael Parsai, Committee Chair

_____

Dr. Diana Shvydka, Committee Member

_____

Dr. John Feldmeier, Committee Member

_____

Dr. Patricia R. Komuniecki, Dean

College of Graduate Studies

University of Toledo

June 2012

An Abstract of

A Novel Device for Delivering Combined Partial Breast Irradiation
and Partial Breast Hyperthermia

By

Todd A. White

Submitted to the Graduate Faculty as partial fulfillment of the requirements
for the Masters in Biological Medical Sciences Degree in Medical Physics

The University of Toledo

June, 2012

Accelerated partial breast irradiation (APBI) is a popular method of adjuvant radiation therapy after tumor resection for early-stage breast cancer due mainly to the reduced total treatment time. Despite the successes of APBI, many patients do not qualify, and local control rates for APBI may be half that of WBI. Improvements to the APBI technique should be sought to allow more patients to qualify and to improve clinical outcomes.

We propose the addition of partial-breast hyperthermia therapy to accelerated partial-breast irradiation (PBHI) to provide additional benefits. A prototype PBHI system was developed at the University of Toledo. The PBHI device uses a removable heating element to heat the balloon fill solution and surrounding tissue.

System feasibility was verified through modeling using the finite-element partial differential equation solver package COMSOL Multiphysics (COMSOL Inc., Burlington, MA). We modeled our balloon as a 6 cm diameter inner sphere within a 20 cm diameter sphere of breast tissue. The temperature at the balloon surface was kept at 46 ^{0}C for one hour. A temperature of 41 ^{0}C is reached at the 1 cm margin of the balloon in approximately 30 minutes.

The attenuation of the PBHI balloon applicator was measured using gafchromic film and compared to a standard Mammosite applicator. The PBHI applicator shows increased attenuation, estimated at 3.5 % radially, with a maximum increase in attenuation of 10% in a small region off the tip of the applicator.

The homogeneity of the balloon surface temperature was investigated during heating at 4 locations on the balloon surface. A temperature gradient of 2 ^{0}C was observed from the top of the balloon (46 ^{0}C) to the bottom (44 ^{0}C) due to convection.

Tissue heating in a porcine tissue model was performed. A balloon temperature of 46 ^{0}C was used to reach a temperature of 41 ^{0}C at 1 cm depth in approximately 30 minutes.

PBHI may expand the patient population qualifying for PBI, or improve local control, thus providing an enhanced treatment option with minimized side effects. The prototype device shows good performance and the potential for a clinically useable PBHI system.

For Gemma and Jennifer Forever

Acknowledgments

I am in great appreciation of the people who have helped me make this thesis a reality. I would like to thank my family always supporting me in my endeavors. I thank Dr. Parsai for his strong guidance and words of wisdom. I would also like to thank the members of my committee their clarity and insight on this project.

I would like to extend thanks to the clinical staff at the University of Toledo Medical Center, particularly Dr. David Pearson and Nick Sperling, for teaching me the clinical aspects of medical physics. I also would like to thank Mr. Sperling for his assistance with many technical components of my research.

Contents

List of Tables

List of Figures

Preface

Those who cannot be cured by medicine can be cured by surgery. Those who cannot be cured by surgery can be cured by fire. Those who cannot be cured by fire, they are indeed incurable. - Hippocrates (470-377 B.C.)

Chapter 1

Review of Partial Breast Irradiation

1.1 Partial Breast Irradiation Defined

Breast cancer therapy has evolved to become dominated by breast conservation therapy. While mastectomy was initially the treatment of choice, clinical trials have proven that for certain qualifying patient groups a combination of breast conserving surgery with radiation therapy yields similar patient mortality rates while lessening the impact therapy has on the patients' quality of life (Bernier 2006). Breast conservation therapy is generally composed of a localized resection of the breast tumor, followed by a course of radiation to either the whole breast or a locally confined radiation therapy treatment delivered using either brachytherapy or an IMRT technique. A standard course of radiation (180 cGy ~ 25 fractions) to the whole breast following a local excision with negative margins has shown an absolute reduction in risk of local recurrence by 19% (Lehman, 2010). For early-stage breast cancer patients, breast conservation surgery and whole breast irradiation have been shown to be equivalent therapy to modified mastectomy and are quickly becoming the standard of care for as much as 70% of early stage breast cancer patients (Sauer, 2006).

Breast conservation therapy is an option for women who meet the qualifying patient group requirements. Several organizations have published recommended

guidelines for the qualifying patient group and these generally include older patients with early stage, low-risk disease in one site, and non-invasive type cancer with negative nodal status (Njeh, 2010). Breast conservation therapy may also be recommended in cases where local therapy is still desired in spite of systemic disease or in cases where more invasive surgery is not recommended.

Partial breast irradiation is defined as a treatment delivering a radiation dose to a locally confined region within the breast, usually limited to the lumpectomy cavity that remains after the tumor is surgically removed with enough excess normal tissue to give clear margins within the breast. Clear margins are determined pathologically by sampling the excised tissue to look for cancerous cells. The sampled area of the excised tissue is small in regards to the amount excised, and the pathologic examination can be done while surgery is underway where time constraints are important. Therefore, although clear margins are defined, there may be residual disease remaining within the breast. This reality, combined with the fact that most recurrences occur within the same quadrant as the initial tumor provides the basis for the use of localized radiation therapy treatments in lieu of whole breast radiation (Lehman, 2010).

Recent clinical trials have shown that for the qualifying patient group, regional partial breast irradiation yields similar local control rates as whole breast irradiation. PBI can be performed using standard fractionation, but has recently seen the popularization of the accelerated partial breast irradiation (APBI) technique. In this method, the patient undergoes radiation treatment twice daily to a dose of 340 cGy for five (preferably) consecutive days for a total dose of 3400 cGy. This APBI technique has been shown to give similar local failure rates as whole-breast irradiation (Sauer, 2006). There are three

general methods currently used for APBI; interstitial brachytherapy, intracavitary brachytherapy, and external beam therapy.

1.2 Partial Breast Irradiation Via External Beam Therapy

External beam therapy has been used routinely for giving boosts to the tumor bed after initial whole breast irradiation. The boost usually consists of a single electron beam blocked to conform to the tumor bed and depth-limited by selecting the appropriate electron beam energy, or by using a pair of conforming photon beams when the tumor extends past the maximum range of available electrons. The tumor bed boost usually follows a standard course of 3D conformal whole breast irradiation, where the tumor with a 1 cm margin is then given another ~1000 cGy. This technique is advantageous as it reduces the amount of healthy tissue receiving unnecessary dose such as the lungs and/or heart, and can also reduce side effects such as radiation-induced fibrosis within the breast itself.

External beam therapy as a primary radiation therapy to the tumor bed is currently delivered using several techniques such as 3D conformal, Intensity Modulated Radiation Therapy (IMRT), or Intra-Operative Radiation Therapy (IORT). Though less common, electrons and proton therapy has also been used as a primary therapy. All the therapies have commonality in that they are typically used to provide APBI treatment after a local excision or lumpectomy is performed to remove the local disease with clear margins. The target is typically prescribed as the tumor bed with a 1-1.5 cm margin to account for setup error, potential residual disease, and patient motion. The advantages of using external beam therapy are that it is non-invasive, can be done with standard equipment

most cancers centers will have, and yields a more homogeneous dose distribution than brachytherapy. The main drawback to external beam therapy is that it likely gives more unwanted dose to healthy tissue over more conformal techniques using brachytherapy. Typical local recurrence rates for APBI given with external beam radiation vary from 1-6% (Lehman, 2010).

1.3 Partial Breast Irradiation Via Brachytherapy

Brachytherapy has been used to treat breast cancer since 1929 when Sir Geoffrey Keynes pioneered implanting radium needles within the breast to treat primary tumors (Polgar 2009). Brachytherapy is defined as a treatment where the source emitting the radiation is placed close to the tumor itself, and is usually accomplished with miniaturized radioactive sources that can be placed directly in the tissue, within a body cavity, or on the surface of the patient. Many of these sources (or many dwell positions when using a single source) are placed in strategic locations within the tumor to produce a highly conformal dose distribution. Brachytherapy has remained a viable treatment option due to the highly conformal nature of the treatment which is accomplished by using a low-energy x-ray, or in some cases electron, source.

Since the initial use of brachytherapy by Keynes, interstitial brachytherapy has been used for breast cancer therapy in the form of radioactivated needles, seeds, and wires that are directly implanted in the tissue, or with miniaturized radioactive sources attached to wires introduced through catheters that are inserted into the tissue. There are three main types of breast cancer therapies that have used interstitial brachytherapy and these include; treating large, inoperable tumors, providing a boost to the tumor bed as an

adjunct to an external beam modality; and most recently, as the primary form of adjunct radiotherapy for early-stage disease (Polgar, 2009).

APBI using brachytherapy was first accomplished in the late eighties and early nineties using the multi-catheter technique (Polgar, 2009). The accelerated treatment schedule, with more than one fraction per day, allows the total dose to be delivered in a shorter period of time which is important for patient quality of life when the patient has catheters implanted within the breast tissue. The multi-catheter technique uses between 10-20 hollow needles that are implanted in the tumor bed volume and margin around the tumor bed. Catheters are introduced through the needles and the needles are removed leaving the catheters remaining in the tissue. The catheters are fixed in place, allowing for patient motion between fractions. A localization method is then performed to allow for a precise treatment plan to be made. Typical prescriptions for multi-catheter APBI are 10 fractions of 340 cGy, or 8 fractions of 400 cGy (Polgar, 2009). Early studies involving APBI yielded poor outcomes when compared to WBI, mainly due to patient qualifying parameters that were not conservative enough. More recent studies have shown that the multi-catheter APBI technique yields similar local control rates to WBI (Polgar, 2009).

The newest development for APBI delivery has come in the form of intracavitary applicators designed to make the APBI treatment process easier, allowing for more treatment centers to offer APBI. These applicators have the general form of an expanding device that forms the resected tumor (lumpectomy) cavity to a quasi-spheroid shape. The applicator has pathways, or lumens to allow for the introduction of a radioactive source via afterloader technique into the breast to deliver the treatment.

Current FDA-approved applicators include the Mammosite single and multi-lumen applicator, the Contura applicator, and the SAVI (Strut-Adjusted Volume Implant) applicator (See Figure 1.1).

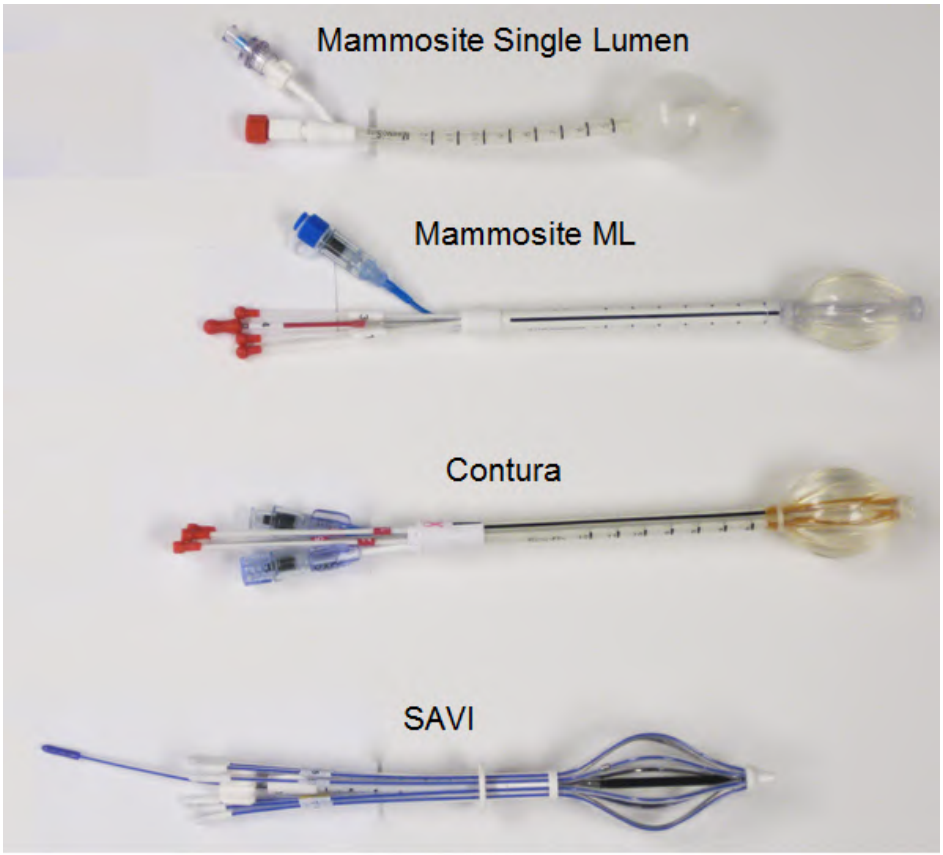

Figure 1.1 Four current FDA-approved PBI applicators; Mammosite single-lumen balloon applicator, Mammosite ML balloon applicator, Contura balloon applicator, and SAVI applicator.

The Mammosite and Contura applicator are similar in construction. These applicators have a balloon on the end that is inflated with saline to conform the cavity to the spherical balloon shape. Both applicators have a one or more lumen for delivery of the radioactive source into the applicator. The resulting spherical lumpectomy cavity provides a convenient geometry for treatment planning and allows for a single dwell position to be used at the center of the applicator, or multiple dwell positions can be used

to shape the dose. Mammosite has both a single-lumen applicator and a multi-lumen (ML) applicator. The Contura applicator is only available as a multi-lumen type applicator. The purpose of the multi-lumen applicators is to allowed for a non-spherical dose distribution that can be used to spare dose to the lung or skin interface. Excessive dose to either the lung or skin can prevent a patient from qualifying for the treatment. Both the Contura and Mammosite ML can provide an approximately 10-15% dose reduction in the axial direction (Detwiler, 2010).

The SAVI applicator uses a significantly different design and is composed of eight peripheral hollow struts and a central lumen, all of which are potential source pathways for delivery of the radiation dose. There is no expanding balloon, and the struts are contracted by the central lumen structure to form a quasi-spherical cavity. This applicator is a significant deviation in design from the expanding balloon-type applicator, and as such has very different dose distribution characteristics. The great advantage of the SAVI applicator is that it can achieve an approximately 50% dose sparing in the axial direction (Detwiler, 2010), which should allow more women to qualify for APBI.

The design of the SAVI applicator can provide a superior dose obliquity, yet new issues arise as a result of this design. First, the sources sit at the edge of the applicator at the skin surface, and therefore the skin surface next to the dwell positions will receive extremely high dose due to the $1/r^2$ fall-off with distance (r) that is a characteristic of brachytherapy. Another issue with the design is that since there is no saline filled balloon, there is an air cavity that may partially fill with bodily fluid and represent a deviation from body geometry used in the initial CT, which will result is small differences in planned and delivered dose. Problems with the SAVI applicator have also

arisen clinically. There have been reports of the source wire piercing the catheter, as well as great difficulty in getting the source wire to transit the struts (NRC, 2011).

1.4 Patient Qualifications for Accelerated Partial Breast Irradiation

A significant lesson was learned from the early APBI trials in that very conservative patient qualifications must be met to ensure that the local recurrence rates are kept in accordance with the traditional whole breast irradiation approach (Polgar, 2009). Several groups have established guidelines for determining patient qualifications including the American Brachytherapy Society (ABS), American Society of Breast Surgeons (ASBS), American College of Radiation Oncology (ACRO), and the American Society for Therapeutic Radiation and Oncology (ASTRO). These requirements can be summarized to include only women of low-risk breast cancer diagnosis as determined by certain criteria: older than 45 years of age, small clinical tumor size (<= 3 cm), negative microscopic margins, minimally-invasive tumor type (Ductal Carcinoma In-situ (DCIS) or invasive ductal carcinoma), negative nodal status, and appropriate relative lumpectomy-breast geometry. This last requirement is important as the relative location of the lumpectomy cavity to the lung-breast or skin-breast interface determines the dose the lung or skin surface will receive. Both the lung and skin surface are generally required to receive less than 145% the prescription dose of 340 cGy per fraction, which generally requires more than 5-7 mm of tissue between the lumpectomy cavity and the skin or lung surface for standard single-lumen balloon applicator brachytherapy. This patient-population limiting factor is precisely the reason for the development of the multi-

lumen applicator design, as it allows for a smaller tissue thickness depending on the amount the applicator can reduce the dose to the interface.

Chapter 2

Review of Hyperthermia

2.1 Hyperthermia as Radiation Sensitizer

The application of heat as a medical therapy has been used for thousands of years with the oldest recorded use found in Egyptian surgical papyrus dated circa 3000 B.C. The earliest medical uses of heat were likely cautiseration and thermal ablation (Van der Zee, 2002). Thermal ablation (heating of tissue to temperatures of 50-70 degrees C) is still a viable medical technique used today for destroying cells as a primary therapy. However, heating of tissue at lower temperatures can also provide a therapeutic effect. Methods of applying heat have included hot water applicators, electromagnetic devices, focused ultrasound instruments, and microwave delivery devices, with most delivery systems surface-based.

Hyperthermia is defined as moderate heating (41-48 ^{0} C) of tissue. Hyperthermia as a primary therapy is an ineffective treatment for cancer, yet it has been shown to increase the effectiveness of other therapies. In particular, hyperthermia is proven to increase the effectiveness of radiotherapy, chemotherapy, and drug uptake in the localized region of hyperthermia treatment. Moderate heating to the tumor concurrent to radiation is proven to increase cell kill by acting as a powerful radiosensitizer, which is of particular interest to our motives (See Figure 2.1). There is no inherent significantly

different action that hyperthermia has on cancer cells over normal cells on the cellular level, however the chaotic nature of cancer growth provides an environment where increased cell death occurs when hyperthermia is applied (van der Zee, 2002)

One of the fundamental biological limitations of radiation treatment is that some cancer cells are resistant to radiation-induced damage. There are three major reasons, namely, variable sensitivity of cells as they undergo mitotic cycle (S and G1 phases which are most radio-resistant), poor tumor vasculature resulting in hypoxic conditions, and cellular repair of sub-lethal damage.

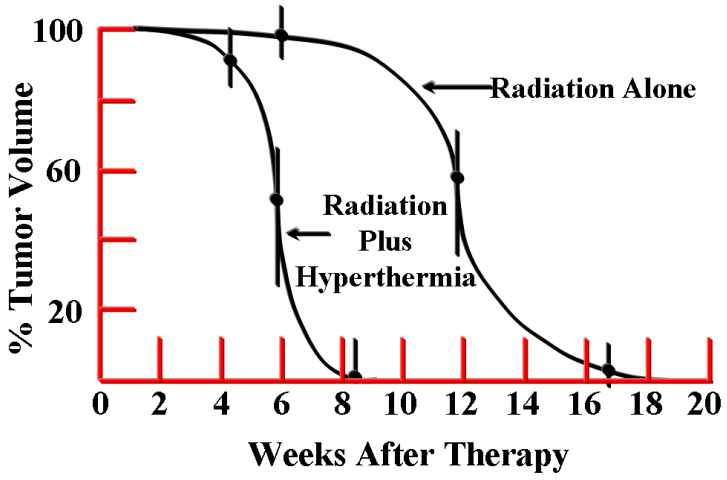

Figure 2.1 An example of the effect of hyperthermia in combination with radiation in treatment of malignant melanoma versus time (Adapted from Chichel et. al, 2007).

Radiation-induced damage to cells works by damaging DNA to the extent that the effected cell undergoes cell death, or can no longer reproduce. DNA is damaged in the radiation interaction by two main actions; direct hits of the double-helix DNA strands by the secondary electrons produced from the radiation interacting with the bodily tissue, and the production of free-radicals within the tissue from stripping of electrons from

atoms. Direct hits to DNA strands will produce single, or double strand breaks. Single-strand breaks within a portion of DNA is termed sub-lethal damage, as the DNA can often repair itself. A double-strand break is seldom repaired and most often results in cellular death, or the cell becoming incapable of replication. The most significant free-radical produced within the body from radiation is oxygen that has been stripped of an electron, which then react with a nearby molecule, often damaging DNA. Hypoxic environments, such as poorly vasculated cancerous tissue, can be as much as 2 or 3 times more resistant to radiation as tumor-rich environments (See Figure 2.2).

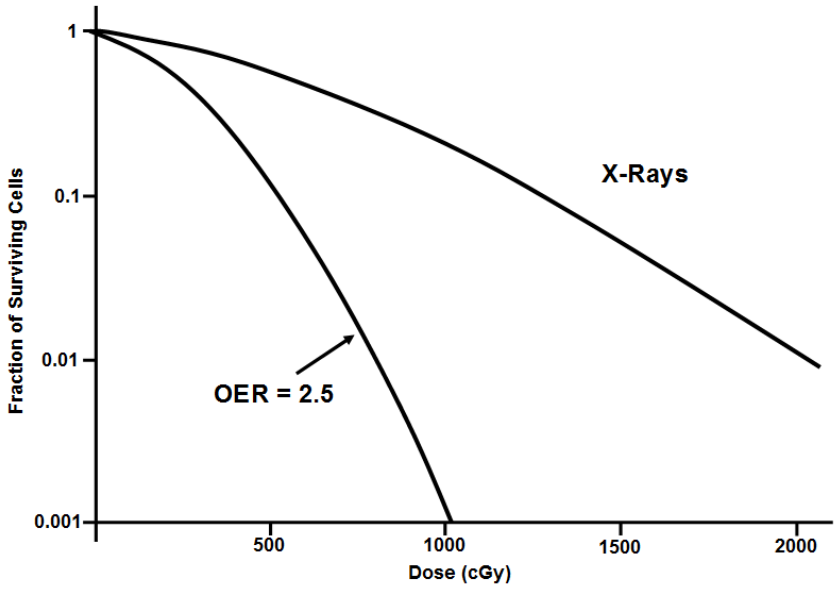

Figure 2.2 Cell kill versus dose for hypoxic and oxygenated cells from *in vitro* laboratory measurements when exposed to x-rays (Adapted from Hall 2006).

Hyperthermia is known to increase blood flow to the heated region, which may provide the mechanism by which hyperthermia lead to improvements in oxygenation within the cancerous tissue, thus increasing sensitivity to radiation treatments. However, this effect can only increase cell kill at most by a factor of 3 as shown by laboratory

measurements, and *in vivo* studies have shown that hyperthermia can enhance cell kill by a factor of between 1.2 up to 5. It is also proven that hyperthermia can restrict the repair of sub-lethal damage, potentially by disrupting proteins (Van der Zee, 2002).

2.2 Measuring the Effect of Hyperthermia

One requirement for standardizing hyperthermia treatments is that the heating effect on tissue is accurately quantified so that the results can be intercompared between trials. One method of describing the amount of heating deposited locally within a tissue volume is thermal dose. The most used quantity to describe thermal dose is that of cumulative equivalent minutes at 43 degrees C or CEM 43 ^{o}C T_{90} (Hall, 2006). More technically, this quantity is the number of cumulative equivalent minutes at least 90% of the monitored points within the target tissue spend at 43 ^{o}C. The temperature of 43 ^{o}C is used as an experimentally determined change in slope occurs for the cell survival curves versus temperature plot at this point, which may represent a difference in cell kill mechanism. The term equivalent is included because a conversion is allowed for the time the tissue was at therapeutic temperatures that were above or below 43 degrees C. One minute for the temperature of monitoring points between the therapeutic threshold and 43 ^{0}C will be equivalent to less than one CEM 43 ^{o}C T_{90}, while one minute for monitoring points above 43 degrees C will be equivalent to more than one CEM 43 ^{o}C T_{90}. The conversion to CEM 43 ^{o}C T_{90} can be accomplished using an established Arrhenius plot, or cell survival curve appropriate for the cell type in study. A rule of thumb is that an increase in temperature by one degree C results in a reduction in the required heating time by a factor of two for an equivalent thermal dose. The major drawback of the

thermal dose is that it applies only to cell death due to hyperthermia alone, with no input for adjuvant radiotherapy, though it may be useful when describing the amount of hyperthermia used in conjunction with radiotherapy. One such study that did just this type of assessment showed that an adjuvant thermal dose of 10 CEM 43 ^{o}C T_{90} yielded a significant local control benefit (Jones et al., 2005).

The measured increase in cell killing when hyperthermia is used in conjunction with radiation requires a different way of quantifying the synergistic effect. An important first step in making the application of heat usable in the clinic is to quantify the effect the heat will have on the radiation therapy. One method to quantify the action of hyperthermia is to apply a factor that is termed the thermal enhancement ratio (TER), which is defined as the ratio of radiation without hyperthermia to that with hyperthermia to give the same biological effect (See Equation 2.1).

$$TER = \frac{Dose\ (cGy)}{Dose\ with\ Adjuvant\ Hyperthermia\ (cGy)} \qquad (2.1)$$

TERs for a heating program lasting 1 hour are shown to have typical values of 1.4 at 41 ^{0}C, 2.7 at 42.5 ^{0}C , and 4.3 at 43 ^{0}C through *In Vitro* laboratory measurements (Hall, 2006). *In Vivo* studies have shown enhancement factors of between 1.2 to 5 (Van der Zee, 2002). It is unlikely, however that the upper end of the TER ratios wll be realized, as laboratory tumors tend to be under other stresses such as nutrient deprivation, which cause them to over-respond to other treatments (Hall, 2006). The proportion of cell kill is related to the magnitude of the temperature, the length of time heating is performed, and the temporal relationship between the heating and radiation therapies (See Figure 2.3) (Horsman, 2007). Clinical studies have shown that maximal TER's are clinically

realized when radiation and hyperthermia are delivered to a tissue simultaneously, or within very close temporal proximity (Van der Zee, 2002, Horsman, 2007).

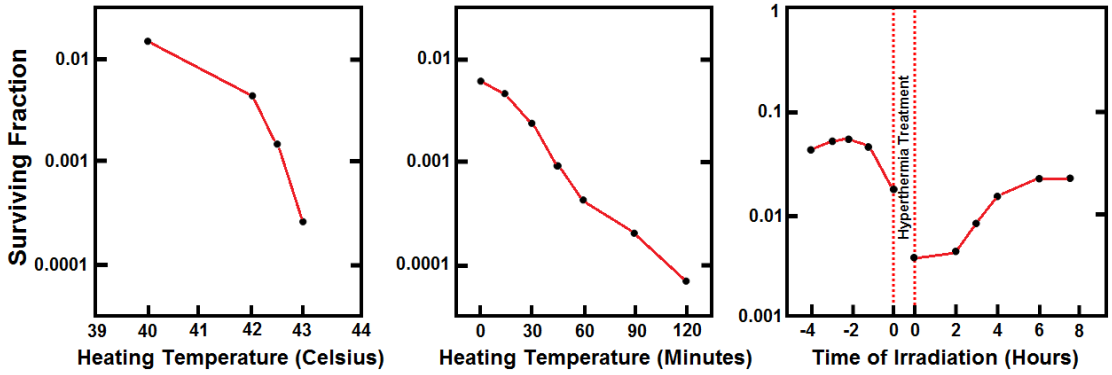

Figure 2.3 Cell survival curves for Chinese hamster cells in culture showing the relationship between cell survival and temperature of heating, duration of heating, and temporal relationship between heating and radiation (Adapted from Horsman, 2007).

2.3 Potential Issues with Hyperthermia

Hyperthermia is one of the most effective radiosensiting agent known, yet it has not been widely adopted in clinical use. The reasons for the reluctance to use hyperthermia as an adjuvant therapy to radiation stem mainly from the difficulty in treatment delivery. In many of the first clinical trials, inadequate treatment methods were used, resulting in disappointing clinical outcomes. These poor initial results resulted in a reduced interest in hyperthermia that has continued until recently renewed interest. Hyperthermia treatment delivery can be complicated by trouble with inhomogeneous heating of tissue, inadequate thermometry, tissue penetration, long treatment times, need for thermal treatment planning system, and labor-intensive nature of treatments.

One problem inherent with hyperthermia described as thermotolerance creates issues when used with typical fractionated radiotherapy treatment regimes. Thermotolerance is defined as resistance of a tissue to cell killing by a subsequent hyperthermia treatment that develops after an initial treatment. This phenomena has been shown to exist due to laboratory experiments where the initial heat treatment was able to produce a magnitude of cell killing that was not repeatable for subsequent heat treatments. The level of thermotolerance that can develop within a cell population is determined by cell type, magnitude of heating, duration of heating, and the time interval allowed between heat treatments (Horsman, 2007).

The issue of tissue heating inhomogeneity has also been addressed. Tissue heating inhomogeneity, and poor heat penetration depth has been a significant problem with surface heating techniques. Internal heating methods such as hot water balloon heating techniques have an advantage over external methods in that the heating device is in contact with the target tissue and does not have to traverse significant amounts of normal tissue to reach the target.

Clinical studies investigating thermotolerance when fractionated hyperthermia was combined with radiation treatments have shown conflicting results. A study measuring thermal enhancement for a single fraction versus a five-day fractionated regimen showed no difference in thermal enhancement. However, both clinical and laboratory studies have demonstrated the existence of thermotolerance (Horsman, 2007).

2.4 Hyperthermia as Chemotherapy Potentiator

Hyperthermia also potentiates the local effects of many types of chemotherapy (See Table 2.1) (Hall, 2006; Van der Zee, 2002). The types of chemotherapy agents that are potentiated by heat include alkylating agents, nitrosureas, and platin analogues. One example of the increased potentiality of Cisplatin for *in vitro* laboratory measurements is given in Figure 2.4.

Table 2.1 List of chemotherapeutic agents and their potentiating effect relationship to heat (Adapted from Hall, 2006).

Effect	**Drug**
Potentiated by heat	Melphalan Cyclophosphamide BCNU Cis DDP Mitomycin C Bleomycin Vincristine
Unaffected by Heat	Hydroxyurea Methotrexate Vinblastine
Complex Interaction	Doxorubicin

This synergistic relationship is especially significant for the agents bleomycin and doxorubicin at temperatures of 43 ^{o}C (Hall, 2006). One explanation for this synergistic relationship is the increased blood perfusion due to local hyperthermia, since blood is the agent carrier. However, there are many possible potentiating mechanisms, and this effect

is not well understood. The enhancement ratio for combined hyperthermia and chemotherapy temperatures range from 1.2 to 10. Not all chemotherapy agents have shown an increased potentiating effect and these include antimetabolites vinblastine, vincristine, and etoposide (Hall, 2006).

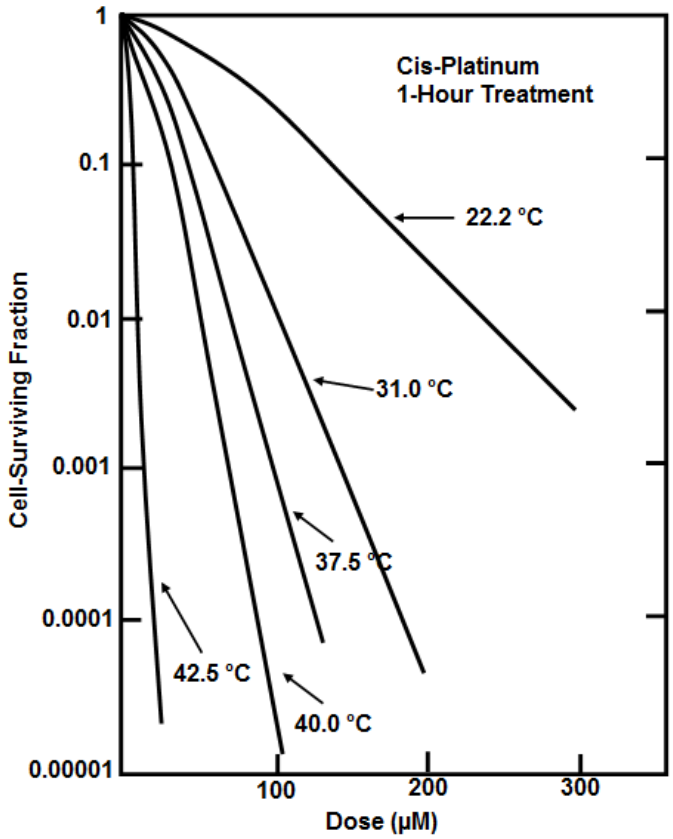

Figure 2.4 Cell survival curve for potentiating of Cisplatin versus several temperatures of hyperthermia (Adapted From Hall, 2006).

2.5 Clinical Trials using Hyperthermia and Radiation

Many randomized clinical trials have been performed to determine the effectiveness of hyperthermia in conjunction with radiation therapy. A wide variety of

heating techniques and regimens have been used, yielding a fairly broad spectrum of results. Despite early trials yielding disappointing results likely due to inferior methods of heating, meta-analysis of the many clinical trials performed to date has shown significant local control improvement in most cases (See Table 2.2) (Horsman, 2007). The fact that a significant clinical improvement is seen despite the wide variety of methods shows the clinical effectiveness of hyperthermia as a radiosensitizer.

Table 2.2 Local-regional control results from a meta-analysis of all clinical trials for thermoradiotherapy (Adapted from Horsman, 2007).

Tumor Site	No. of Trials	No. of Patients/Lesions	Radiation Alone (%)	Radiation + Hyperthermia (%)	Odds Ratio (95% C.I.)
Advanced Breast	2	143	67	68	1.06 (0.52 - 2.14)
Chestwall	4	276	38	59	2.37 (1.46 - 3.86)
Cervix	4	248	52	77	3.05 (1.77 - 5.27)
Rectum	2	258	9	19	2.27 (1.08 - 4.76)
Bladder	1	101	51	73	2.61 (1.14 - 5.98)
Prostate	1	49	79	81	1.16 (0.28 - 4.77)
Melanoma	1	70/128	31	56	2.81 (1.36 - 5.80)
Head & Neck	5	274	33	51	2.08 (1.28 - 3.39)
Mixed	3	442	34	39	1.24 (0.84 - 1.82)
All Trials	23	1861	38	52	1.80 (1.50 - 2.16)

CI is Confidence Interval, All results are for locoregional control

The odds ratio found in Table 2.2 for the combination of hyperthermia and radiation in treating advanced breast cancer appears low at 1.06. This is misleading, however as the 95% confidence interval incorporates a large range, illustrating that the effectiveness of the therapy varied according to trial. A breast cancer specific consensus report of the results of five randomized clinical trials for thermoradiotherapy of superficial localized breast cancer by Vernon et. al, 1996 showed an overall advantage of local control for hyperthermia plus radiation of 59% versus radiation alone of 41% at two years. A survival benefit was not shown for these trials due to the fact that much of the

patient population had significant metastatic disease. Another clinical trial report by Overgaard et. al. 1995 yielded a local control rate of 46% for the combined arm versus 28% for the radiation alone arm. These results show that a significant improvement of local control can be obtained using hyperthermia in combination with radiation. The proven advantage of hyperthermia plus radiation is the reason that hyperthermia is seeing a resurgence of interest in the research community for a variety of cancer types.

2.6 Partial Breast Irradiation plus Partial Breast Hyperthermia Rational

We propose the addition of partial breast hyperthermia therapy to standard partial breast irradiation therapy that is currently used in breast conservation therapy. The addition of hyperthermia to partial breast irradiation can offer several advantages over radiation therapy alone. The improvements to partial breast irradiation can be accomplished through either an increased local control rate or a significantly reduced dose with the same control rate due to the addition of hyperthermia.

Partial breast irradiation is a minimalist therapy that treats only a portion of the breast to high doses of radiation (3400 cGy). Many patients do not qualify for this therapy due to the potential for significant skin doses or lung doses. As seen in laboratory and clinical trials, the potential for local control improvements due to the addition of hyperthermia treatments could be a factor of *at least* 1.4 depending on the effectiveness of the hyperthermia regime. If the same local control rate due to radiation therapy alone was accepted, then the total dose could be reduced, allowing for more patients to qualify for the therapy. In addition to more patients qualifying for this

therapy, radiation-induced side effects such as fibrosis, skin erythema, and secondary cancers could be reduced.

One can investigate the potential increase in effectiveness of the cancer treatment through the biologic effective dose equation, which is derived from the linear-quadratic cell survival model (See Equation 2.2) (Hall, 2006).

$$\frac{E}{\alpha} = (n\,d)\left(1 + \frac{d}{\alpha/\beta}\right) \qquad (2.2)$$

The term E/alpha is called the biologic effective dose (BED) and can be used to intercompare different dose fractionation schemes. The term n is the number of fractions, the term d is the dose per fraction, and the alpha/beta term represents the component of early or late effects. Breast cancer cells can have tumor-doubling times of greater than 100 days, responding similar to late-responding tissue. The alpha/beta ratio for breast cancer has been experimentally determined at approximately 4 Gy (Theberge et al., 2011). We perform a calculation of BED for the standard APBI treatment and use an alpha/beta of 4 Gy, with 10 fractions of 340 cGy. From these values, and using Equation 2.2 we find a BED of 6290 cGy. Now, if we assume a thermal enhancement ratio for the hyperthermia treatment of 1.6, our effective fractional dose becomes 5.44 Gy, and keeping all other factors the same, we find a BED of 12840 cGy (See Equation 2.3).

$$\frac{E}{\alpha} = (10\,fx \cdot 544\,cGy)\left(1 + \frac{544\,cGy}{400\,cGy}\right) \cong 12840\,cGy \qquad (2.3)$$

The resulting hyperthermia plus radiation BED is over twice the original BED. The higher BED should translate into higher local control rates, although it is difficult to quantify increases in local control due to higher BED.

However, we could probably not be able to use the same accelerated treatment schedule due to thermotolerance, which would require a spacing out of the treatments, and the treatment schedule would have to be redesigned to maximize the benefit of hyperthermia while minimizing the effect of thermotolerance. One possible treatment scenario we have calculated as twice per day fractions of 220 cGy with hyperthermia delivered during the morning fraction only. This schedule would be spread out over a two week duration with every treatment followed by a two day break to allow for spacing of treatment days to reduce thermotolerance. The extended treatment duration should be negligible, since the tumor doubling time for breast cancer is typically very long (>100 days) (Hall, 2006). If we assume that we can achieve a 1.6 TER using this technique, the effective fractional dose delivered will be approximately 352 cGy. We can then calculate the effective biologic dose for 10 fractions to be 6620 cGy, which is 5% larger than the standard regime effective biologic dose of 6290 cGy (See Equation 2.4).

$$\frac{E}{\alpha} = (10\,fx \cdot 352cGy)\left(1 + \frac{352\,cGy}{400\,cGy}\right) \cong 6620cGy \qquad (2.4)$$

Caution should be exercised, however, as this simple model does not include a method for comparing such different treatment durations.

Assuming our suggested treatment schedule to be effective and correct, we can then translate our treatment schedule into implications for the required balloon surface to

skin distance, which for the current treatment schedule is 7 mm or greater. The smaller the balloon diameter used, the more significant the balloon to skin distance becomes as the skin surface located more on the steep dose gradient for the exponential decay that is a feature of brachytherapy. This means that we can use the smallest expected balloon diameter as the limiting case for skin distance. The accepted current treatment is to prescribe fractions of 340 cGy to 1 cm distance from the balloon surface, and not allow the skin to exceed 145% of the prescription, or 493 cGy. The 7 mm balloon to skin surface appears to be a rather conservative estimate; assuming point source and isotropic geometry, applying the inverse square law, and correcting for attenuation due to the extra 3mm of tissue, we find that the dose to the skin for a 40 mm in diameter balloon to be 433 cGy, or approximately 127% of the prescription dose (See Equation 2.5). Attenuation due to tissue is estimated to approximately 1% per mm of tissue as predicted by linear attenuation coefficients for tissue, and density of breast tissue of 0.92 g/cm^3.

$$Skin\ Dose = 340cGy \cdot \left(\frac{30}{27}\right)^2 \cdot \frac{1}{0.97} = 433cGy \qquad (2.5)$$

The limit of 145% of the prescription is not met until an approximately 5.5 mm balloon-to-skin distance for a 40 mm diameter balloon. The 40 mm balloon diameter corresponds to the smallest Mammosite applicator size. Lumpectomy cavities are normally at least 40 mm in diameter, with the smallest lumpectomy cavities around 30 mm (Jadwiga, 2007).

The fractional dose of 220 cGy using our potential hyperthermia regime described above can be analyzed to determine our balloon-to-skin thickness limits as well. If we keep intact the fractional skin dose limit of 145% of 340 cGy, or 493 cGy, we find for a 40 mm diameter treatment balloon that the skin dose limit is 145.1% of 340 cGy only

when the balloon-to-skin distance is 1 mm. Since this balloon-to-skin distance will likely only prohibits the most extreme cases from treatment, our treatment regime essentially eliminates the balloon-to-skin distance requirement from preventing women who meet the other APBI requirements from treatment.

There are several other characteristics of our treatment method that merit discussion. One common problem with hyperthermia treatments is the heterogeneous distribution of heating within the tissue. This problem is greatly alleviated by using an intracavitary-style applicator as the heat source is located directly adjacent to the target tissue, placing the hottest portion of the treatment within the target tissue. This thermal gradient effect exists with our applicator system, with the tissue directly adjacent to the applicator receiving a higher temperature. Therefore, along with a thermal gradient, there will exist a thermal dose gradient with the highest thermal dose near the applicator and rapidly falling moving away from the applicator. The hyperthermia treatment can be designed so that the 1 cm radiation prescription point still receives an adequate hyperthermic (>41 ^{o}C) temperature. However, there exists an argument that this fall-off in thermal dose is not a significant problem. The goal of the radiation treatment is to 'mop-up' any remaining microscopic disease not evident during the resection. A single tumor typically propagates from a single cancerous cell, and can only grow outward. Because of this nature of cancer, the probability of microscopic disease existing within the normal tissue as you move away from the excised tumor bed decreases with distance in a single-focus disease such as those treated with breast conservation therapy. Therefore, it may not be significant that there will exist a thermal dose gradient with our therapy, just as there is a radiation dose gradient.

Another potential issue with our treatment method is that normal tissue may react to the thermal dose similar to cancerous tissue which may negate the benefits of the reduced radiation dose to the normal tissue. Results of clinical studies have shown that both early and late effects due to the addition of hyperthermia to radiation therapy are extremely rare or not observed (Horsman, 2007). Additionally, active cooling methods could be used to reduce the temperature of sensitive normal tissue such as the skin and the lung. Externally applied cooling techniques can be used on the skin, and cold-air inspiration could be used in the case of the lung, to reduce the temperature of the tissue, thus protecting it.

2.7 Partial Breast Irradiation plus Partial Breast Hyperthermia Treatment Delivery System Requirements

A treatment system for delivering nearly concurrent partial breast hyperthermia and partial breast irradiation (PBHI) requires that certain design criteria are met. Any PBHI system must be capable of delivering the radiative and hyperthermia treatments concurrent, or as close as possible to allow for maximal TER for the hyperthermia treatments. Our PBHI system meets this requirement through the use of a balloon-type applicator that can deliver both hyperthermia and radiation therapies. This is accomplished by means of a single central lumen that a removable miniaturized resistive heating element can dwell within, heating the balloon fill solution to transfer heat to the surrounding target tissue. Once the hyperthermia treatment is delivered, the heating element is removed and a transfer tube can be inserted in its place allowing for the

introduction of the radiative source, while the fill solution and surrounding tissues are still under hyperthermic conditions.

Another requirement that must be met by a PBHI system is that the tissue must be heated in a controlled, consistent manner. Our PBHI system accomplishes thermal control through the used of a feedback loop system. The feedback loop consists of an imbedded thermocouple within the applicator itself that delivers the temperature of the fill solution to a computerized control system. The control system in turn controls the current delivered to the resistive heating element, closing the loop. The control system allows for a consistent temperature to be maintained within the applicator to allow for repeatable treatments to be delivered. This method does not ensure homogeneous heating of the fill solution, however, and it will be shown that this is one of the potential issues with the system as it is currently designed.

A third requirement that must be met by a PBHI system is that there is a method for ensuring the target tissue is heated to hyperthermic temperatures. This has been accomplished in the past by using *in vivo* thermometry. This type of invasive thermometry can be used with our system, however it may be possible to create treatment duration tables based on computer modeling and/or initial trial thermal measurements.

Chapter 3

Preliminary Modeling in Comsol

3.1 Introduction to Comsol

Preliminary modeling of the applicator was used to ensure that the thermal demands on the applicator to deliver appropriate thermal dose to the target tissue were possible to achieve with available resources. Modeling of the demand required by the heater also allowed for some determination of the specifications required of the miniaturized heater and heating control system. *A priori* knowledge of the requirements of the components also reduced wasted time and money that may have occurred using trial-and-error methods. The modeling program that was chosen is the heat transfer module of the finite-element modeling program COMSOL Multiphysics (Burlington, VT).

Finite-element modeling is a way of simulating a physical process within a virtual environment by breaking up the volume of interest into many small interconnected nodes. Each node acts upon an input from an adjacent node using a set of instructions governed by mathematical solutions to physical processes. The result of this mathematical algorithm is then the input for the next adjacent node, etc. An error analysis is performed for the model with respect to how well the model fits the input parameters, and the model is adjusted until a prescribed degree of fit is found. The user

can control the model by adjusting certain boundary conditions, adjusting the mathematical algorithm, and by adjusting parameters used to adjust the virtual model to reflect physical properties such as density, conductivity, etc., of the physical object the user is modeling.

The nodes of the finite element model used in the heat transfer module use mathematical algorithms based on the first law of thermodynamics, or conservation of energy. The general, steady-state form of the equation solved by the heat transfer module is given in Equation 3.1.

$$\rho C_\rho \frac{\partial T}{\partial t} + \rho C_\rho u \cdot \nabla T \equiv \nabla \cdot (k \nabla T) + Q \qquad (3.1)$$

Where ρ is density, C_p is the specific heat capacity, T is the absolute temperature, u is the velocity vector, k is the thermal conductivity, and Q is the heat source. This equation ignores viscous heating and pressure work and is valid for fluids. If you remove movement from the equation by removing the velocity vector, you get the steady-state equation for heat transfer in solids (Equation 3.2). A time-varying form of this equation is used in our model (Comsol, 2006).

$$\rho C_\rho \frac{\partial T}{\partial t} + \nabla \cdot (-k \nabla T) \equiv +Q \qquad (3.2)$$

The heat transfer equations used in Comsol were solved directly using the PARIDISO solver. The PARADISO software is a widely used, memory efficient and robust solving package that is used to solve large, sparse matrices. This solver package

allowed for quick solutions for our model, which consisted of a large number of finite elements.

3.2 Heat Transfer Modeling Parameters

The heat transfer module allows for two or three-dimensional modeling of the applicator device. Though two-dimensional modeling would have suited the purpose, three-dimensional modeling was chosen to allow for further complexity to be implemented in the model if it became necessary. The model is very simple and consisted of a 6 cm diameter sphere filled with water surrounded by a 20 cm diameter phantom modeled with appropriate thermal properties for breast tissue (See Figure 3.1).

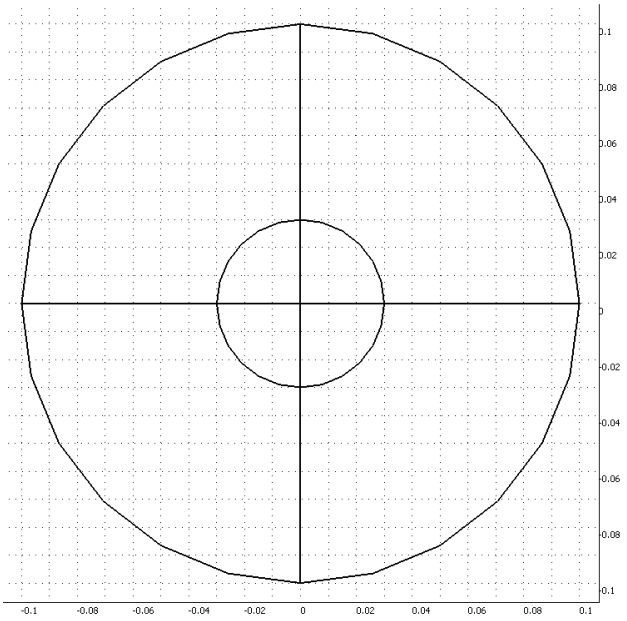

Figure 3.1 A two-dimensional representation of the construction of the heating model in Comsol. The center balloon is six cm in diameter and the surrounding tissue phantom is 20 cm in diameter (units in meters).

The three-dimensional model space was broken into a fine mesh of 282,552 elements to improve the resolution of the results. A rendering of the mesh is shown in Figure 3.2.

Modeling parameters for the phantom include thermal conductivity, specific heat capacity, and density of the material. The properties for water are well known and easily available. The parameters for breast tissue are not as well-defined, vary from person to person, and as such, a literature review was undertaken to find appropriate values that have been used in past modeling studies. The parameters used for the model are given in Table 3.1 below. The thermal properties used in our modeling study were taken from a thermal modeling study of breast tissue by Y. He et a., 2006. Our model was also tested for sensitivity to these parameters which will be further discussed below.

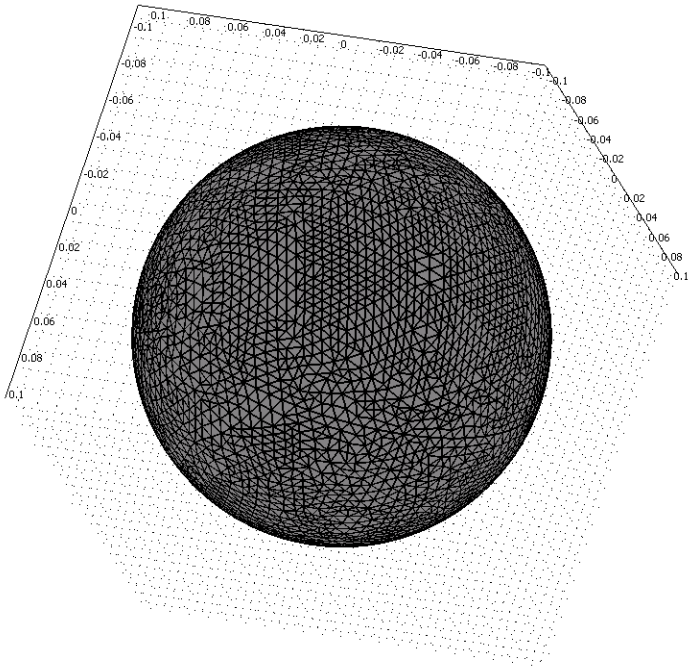

Figure 3.2 Three-dimensional representation of the mesh of the finite element heating model in Comsol (units in meters).

Table 3.1 List of thermal properties used for finite element model.

Material	Density (kg/m)	Thermal Conductivity (W/m k)	Heat Capacity (J/kg K)
Breast	1020	0.4	4350 (or 3689)
Water	1000	0.6	4181

Also necessary for the model is to define the initial thermal boundary conditions. The internal sphere was initially held at the upper end of the hyperthermic temperature range noting that thermal properties of the breast tissue will create a steep thermal gradient, and to allow for the deepest penetration of the heat possible. This temperature for the inner water sphere was kept at 46 degrees Celsius. The breast tissue was initially set to body temperature, 37 degrees Celsius. The boundary between the spheres was defined as an open boundary, while the external breast sphere boundary was kept as an insulating boundary. The insulating boundary was considered appropriate even though the skin cools the body through perspiration and evaporation, the highly insulating effect of the thermal properties of the breast phantom should make this cooling effect minimal.

3.3 Preliminary Modeling Results

The thermal distribution of the model previously described was solved at increments of time up to 90 minutes of heating by the central balloon to understand how hyperthermic conditions can be imposed in the tissue. Since the radiation therapy is prescribed to 1 cm axial distance from the edge of the balloon, we seek to deliver a hyperthermic dose to this isoline to remain consistent with current prescription technique for PBI. The result of our heating method at 30 minutes is shown in the cross-section of our phantom given in Figure 3.3.

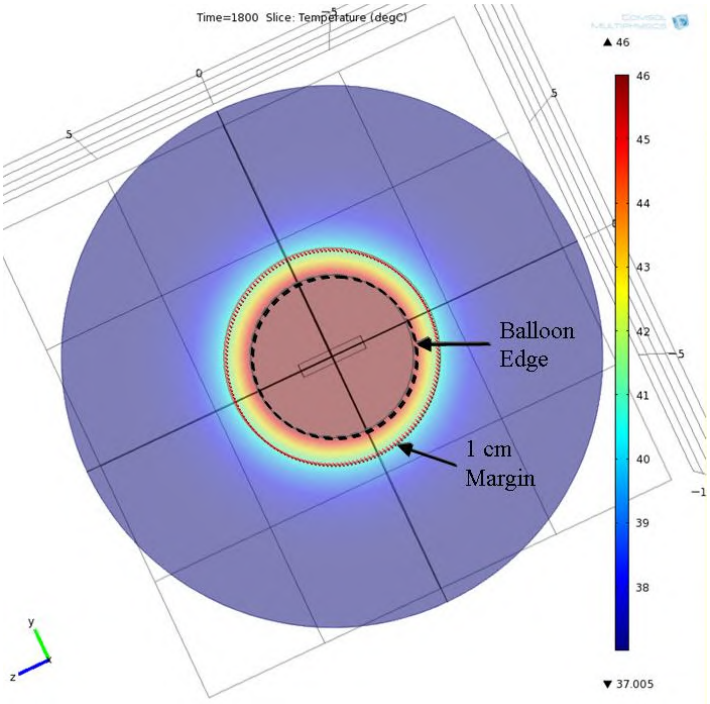

Figure 3.3 Results for 30 minutes of heating. The 1 cm margin is approaching hyperthermic temperatures. A very steep thermal gradient exists axially from the center of the balloon.

The cross section of the model at 30 minutes shows the 1 cm prescription margin approaching the hyperthermic temperature range. Also evident is the steep thermal gradient radially from the edge of the balloon into the tissue phantom. These results are encouraging in showing that the proposed system will be able to deliver a hyperthermia treatment within a reasonable and clinically realistic time frame. We can look more subjectively at the model results by looking at temperature profiles through the model as a function of distance for several different times (See Figure 3.4).

The temperature profiles in Figure 3.4 show the radial thermal distribution from the balloon edge for several time durations. The initial time zero model is peculiar, as it does not agree with the initial conditions. The Comsol program does not appear to like discontinuities, as the thermal discontinuity that should appear at the balloon edge at time

zero is averaged over, decreasing the temperature at the inner edge of the balloon and increasing the temperature at the outer edge of the balloon. This discontinuity remains despite the type of algorithm used to solve the problem. The error can be reduced by increasing the nodal density near the balloon edge, however it cannot be removed. Later time periods show similar temperature distributions regardless of the time-zero model error magnitude, so it appears that the resulting later time thermal distributions are not affected by the time zero model to a significant extent.

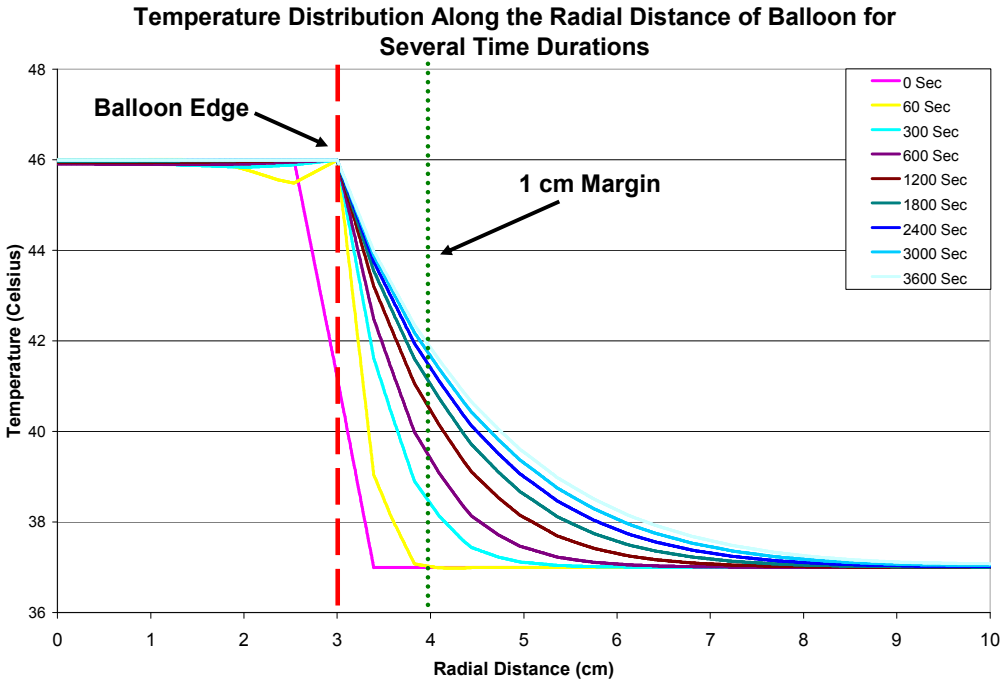

Figure 3.4 Temperature profiles at various times for the model based on thermal properties of breast tissue. The center balloon is held at 46 degrees Celsius.

The profiles in Figure 3.4 also show that the effectiveness of the balloon at heating the tissue decreases as the tissue temperature is raised, and the two volumes become closer to thermal equilibrium. In the first 20 minutes the temperature at 1 cm is

raised nearly 3.5 degrees, while another 40 minutes of heating only raises the temperature at 1 cm another 1.5 degrees.

One important physical characteristic that can effect the thermal response of tissue to hyperthermia applications is blood flow. In the interest of simplicity for our preliminary modeling, we ignore blood flow. Comsol does have a Bioheat transfer module that can incorporate blood flow into the model. The Bioheat transfer module incorporates blood flow into the model by using a simple linear term that reduces the heat in the system proportional to the amount of blood flowing through the volume. This type of model may not adequately describe the actual conditions within the breast. In our system, blood that is near to the balloon applicator will heat up, and will consequently act as a heating component of the tissue as it travels away from the applicator. There may well indeed be a negative total reduction of heat within the system, however due to the blood further heating the system, there may also be a reduction in the steep thermal gradient that exists around the applicator. This flattening out of the thermal gradient could reduce the time required for the treatment delivery to occur.

Parameter perturbation was performed to investigate how the resulting thermal models responded to variations of the three physical characteristic parameters used to describe the thermal properties of breast tissue, density, heat capacity, and thermal conductivity. In general, the variation of these parameters within the range available within the human body produce relatively small changes (less than 1 ^{0}C) in the resulting thermal distribution of the resulting models. The three parameters that were investigated were density, heat capacity, and thermal conductivity.

Densities within the human body range from 930 kg/m^3 for fat to 1900 kg/m^3 for bone. The densities that are relevant for our applicator are even more limited, since we are mainly interested in soft tissue, bone can be eliminated. In this case, the density range applicable is from approximately 930 kg/m^3 for fat to 1100 kg/m^3 for blood. The density we used for our model was 1020 kg/m^3 for the breast tissue phantom. Along with this value, we modeled the thermal distribution for a breast phantom with density of 820 kg/m^3, and a density of 1220 kg/m^3. The results are plotted in Figure 3.5.

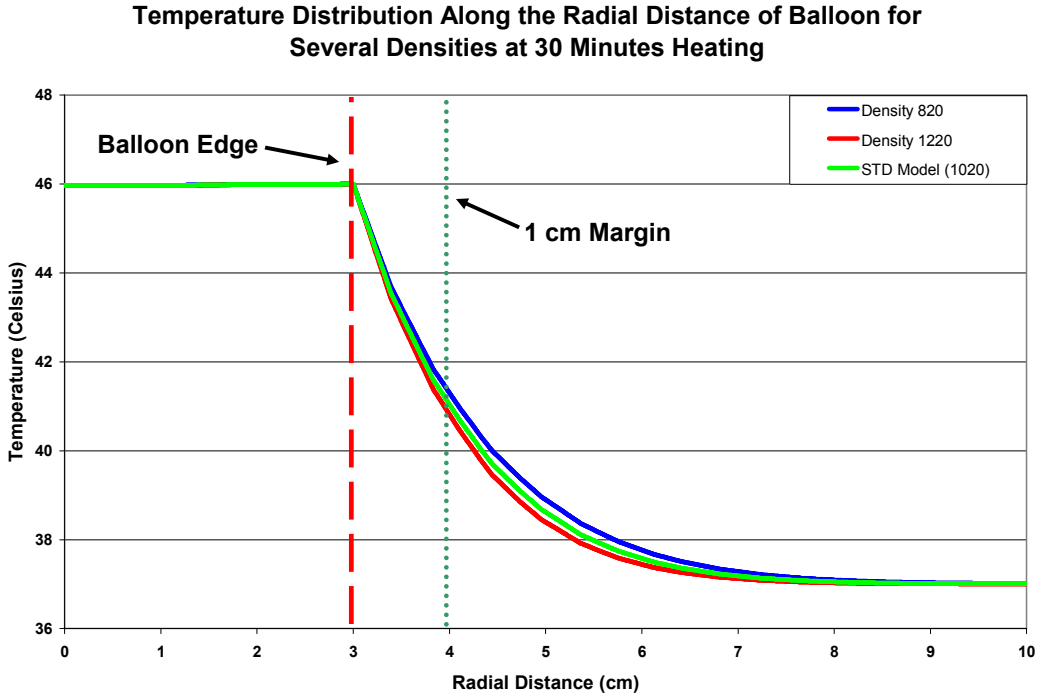

Figure 3.5 Temperature distribution along the radial profile of the model at 30 minutes duration of heating.

The wide range of densities used for the modeled data in Figure 3.5 represent the endpoints of the range of densities of concern, as the actual densities within breast tissue should have a much smaller range than the endpoints given here. The difference in the

resulting thermal distribution within the model for the range of densities is very small. At a duration of one-half hour, the difference in temperature at the 1 cm margin is approximately 0.5 ^{0}C. Since this temperature difference is very small, it is therefore reasonable to use the published value of 1020 kg/m^{3} for the breast tissue modeling. Further implications are that the variations of breast density in the female population is likely insignificant on the resulting thermal distribution induced within breast tissue due to hyperthermia measurements over the duration of a typical hyperthermia treatment.

Specific heat capacity within the soft tissue of the human body range from approximately 2770 kJ/(kg K) for fat to 4200 kJ/(kg K) for skin. A range of heat capacities were modeled while keeping all other parameters the same, similarly to the perturbation modeling for the density range. The results are shown in Figure 3.6.

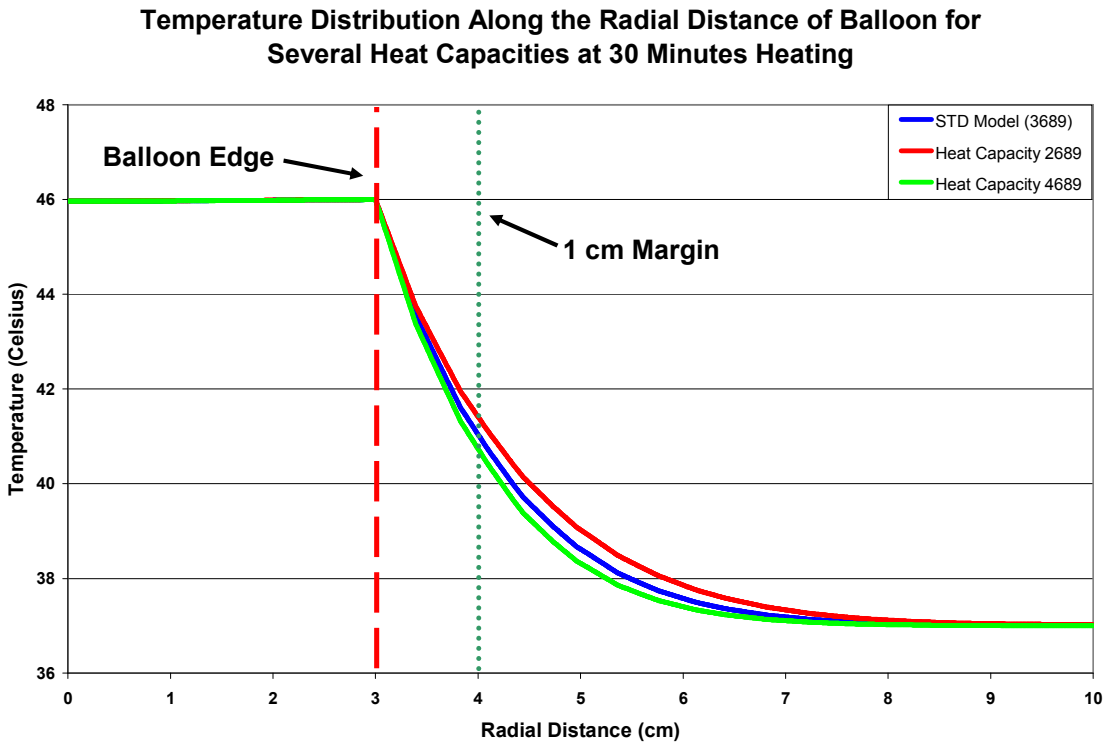

Figure 3.6 Three solutions for the model shown at heating duration 30 minutes.

The difference between the resulting thermal distribution profiles for the range of heat capacities is more significant than the results for the variation in densities, but the difference is again small. At the 30 minute duration the profiles are given for, the temperature difference between the heat capacity endpoints is approximately 0.7 ^{0}C. Again, the variation in heat capacities of breast tissue among the female population is likely very small compared to the range of heat capacities modeled. Due to this fact, heat capacity variations are likely insignificant and has little impact (less than 0.5 ^{0}C) upon hyperthermic treatments of breast tissue. It is also unlikely that variations of density and specific heat capacity within breast tissue yield significant inhomogeneity of the resulting temperature distribution due to hyperthermia treatments.

The third parameter used in the model is the thermal conductivity, and as might be expected, this parameter is the most important of the three in determining the shape of the thermal gradient in the range of thermal conductivities within tissue. Thermal conductivities within soft tissue range from 0.2 W/m for fat to 0.5 W/m for glandular tissue. Though breast tissue consists of mostly fat, a wide range of thermal conductivity values have been used to model thermal parameters within breast tissue, from 0.2 W/m (similar to fat's value), to 0.4 W/m. There may also be a discrepancy between thermal conductivities measured *in vitro* versus measurements made *in vivo*. The value we used for thermal conductivity was estimated to be approximately 0.4 W/m through *in vivo* measurements (Gautherie, 1980). A parameter perturbation was also performed for a range of thermal conductivity endpoints from 0.2 to 0.6 W/m, similar to that performed for the other two parameters (See Figure 3.7).

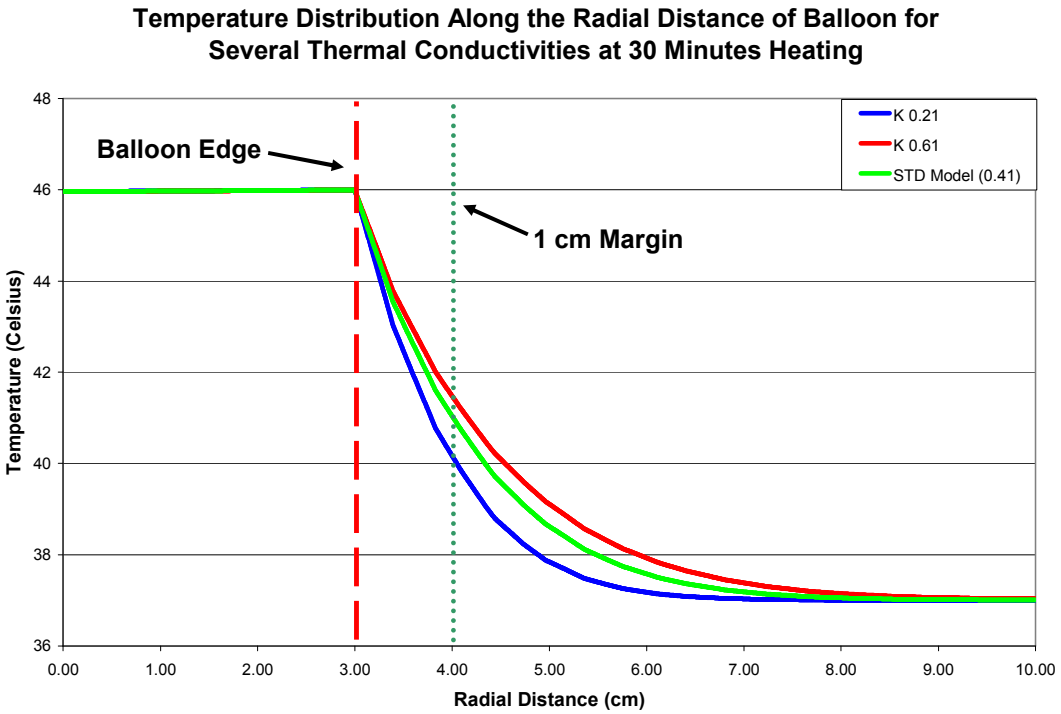

Figure 3.7 Modeling results for three thermal conductivities. Higher thermal conductivity results in higher heating of tissue.

The modeling results shown in Figure 3.7 show a 1.2 ^{0}C difference at the 1 cm margin between the thermal conductivity endpoints. It is not likely for the thermal conductivity to vary this widely in the patient population, but it may vary from 0.2 W/m (fat) to 0.5 W/m (gland) within the tissue itself which could lead to an inhomogeneous heat distribution within the breast. However, the thermal conductivity of cancerous tissue has been reported as similar to that of glandular tissue, indeed most breast cancers are glandular in nature. In this case, heterogeneous heating of the breast may be an advantage, preferentially heating the cancerous tissue, thus selectively treating the treatment target to a higher, more effective temperature.

3.4 Conclusions from Modeling

The preliminary modeling results show that the applicator will likely be able to deliver an effective treatment within a clinically realistic time. The goal of the applicator to meet the modeled results is to hold a homogenous temperature of 46 ^{0}C within the balloon fill solution so that the tissue is homogeneously heated. The most significant tissue characteristic driving the thermal gradient is the thermal conductivity. Variations of thermal conductivity within the breast may give rise to inhomogeneous heating of the tissue, however the residual tumor within the treatment volume may preferentially heat to a higher degree than much of the breast, as glandular tissue has a higher thermal conductivity than other types of tissue.

Chapter 4

Prototype Construction

4.1 Applicator Design

The PBHI applicator design is based on a typical single-lumen balloon type applicator that uses a balloon to expand the lumpectomy cavity into a quasi-spheroid shape, and has a central lumen to allow for the introduction of the source of treatment. The PBHI applicator has a maximum balloon radius of 3 cm perpendicular to the central lumen. The central lumen within the balloon is 4 cm long, assuming 5 mm dwell position length, allows for 8 dwell positions within the balloon itself. The central lumen must also have a wider internal diameter to allow for the introduction of our miniaturized heating element, which has an external diameter of 3.175 mm (1/8 inch). Therefore the internal diameter of the central lumen is slightly larger than 3.175 mm. The miniaturized heating element is removable, which allows for the introduction of a transfer tube to deliver the radioactive source. The transfer tube for the radioactive source is much smaller than the heating element, however, so a centralizer must be attached to the transfer tube to keep it properly aligned within the central lumen. During our testing, we simply used thin (~1-2 mm) strips of tape rolled around the transfer tube.

Our applicator must meet additional criteria since it is used to deliver hyperthermia treatments. One such criteria is that the central lumen of the applicator

must be thermally conductive to allow for the transfer of heat from the heating insert to the fill solution. To meet this goal, the portion of the central lumen within the balloon where the heater insert rests is constructed out of aluminum. Aluminum has a very high thermal conductivity (240 W/(m K)), while also having relatively low density, low x-ray attenuation compared to other metals, and is cheap and easy to machine. Aluminum does attenuate radiation more than the typical plastic construction of PBI applicators, and as such, the additional attenuation will also be investigated. The aluminum tube of the central lumen is designed to be 3.0 cm long, with a 6.35 mm outer diameter and 3.18 mm inner diameter. A diagram showing the final dimensions of the central lumen is shown in Figure 4.1.

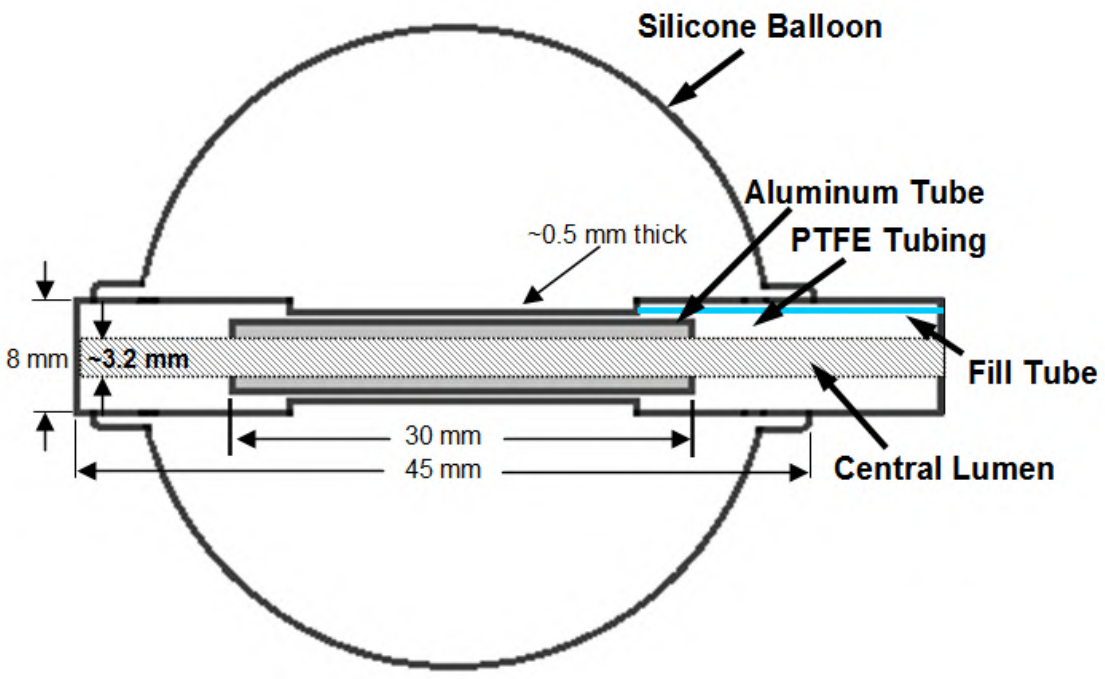

Figure 4.1 Schematic of balloon construction dimensions.

The balloon we used to construct our applicator was carefully removed from an existing PBI applicator device, as it was there was no other good option available, and would make comparison of our PBHI device to an existing PHI applicator easier. The balloon material is most likely silicone, a material that is highly elastic, and relatively resistant to heat (up to 250 ^{0}C).

Though silicone is heat resistant, it was decided to abut the central aluminum lumen with a low thermal conductivity lumen to act as thermal insulation for the balloon material, as well as the patient. Several materials were initially tested for use as thermal insulation. The material is required to have low thermal conductivity, available in tube-form in sizes similar to the central lumen to allow for introduction of the miniaturized heater and the radiative source. The insulative material is also required to be easily machined, and able to adhere to the aluminum tubing, which the first choices of material failed. Initially, fused silica quartz tubing was tried as the abutting thermal insulative tubing to the central aluminum tubing, due to its very low thermal conductivity (~1.4 W/m). This tubing was adhered to the ends of the aluminum using high temperature epoxy. The adhering of the tubing failed however, as the surface area (~0.24 cm^2) of the ends of the small tubes was not enough to result in the desired strength. Additionally the fused silica tubing is relatively fragile, and would chip and crack easily. This lead to the determination that a aluminum oxide ceramic might have higher strength with similar insulative properties (~18 W/m). This tubing is less brittle than the silica tubing, however the same difficulty in adhering the ceramic to the aluminum was encountered as adhering the silica to the aluminum.

The final construction settled on using plastic polytetrafluoroethylene (Teflon) tubing. PTFE tubing has a relatively high heat resistance (melting point 327 ^{0}C) and a very low thermal conductivity (0.25 W/m). PTFE does have one significant drawback, in that it is very difficult to bond, since it is "non-stick". The central lumen was redesigned to circumvent this issue by providing maximum surface area. Instead of only abutting the ends of the aluminum lumen with PTFE tubing, the aluminum tubing was abutted by the same size PTFE tubing, and also a thin walled PTFE tubing encases the aluminum tubing. To reduce the impact of encasing the aluminum tubing with the very low thermally conductive PTFE tubing, a 2 cm length of the PTFE tubing covering the aluminum tubing was etched away to reduce the thickness of the PTFE covering the aluminum.

The central lumen was constructed using a cyanoacrylate (superglue) with an activator solution formulated specifically for hard-to-bond plastic surfaces. The balloon was bonded to the ends of the central lumen using the same cyanoacrylate, however a reinforcement method was used to ensure proper water-tight adhesion. Once the balloon was bonded to the ends of the applicator, a monofilament polymer line was wrapped around the balloon ends, tied, and the same cyanoacrylate was used to form a coating over the line wrapping. This construction method reinforces the connection between the balloon and lumen, preserving the water-proof construction especially when the balloon is filled, which stresses the balloon-lumen contact. The final prototype PBHI applicator is shown in Figure 4.2.

The thermal delivery system requires a feedback loop to inform the heater when to heat and to what degree. The applicator was fitted with a thermocouple to provide this feedback information. Initially, the thermocouple was fitted to the exterior of the

balloon. In later versions, the thermocouple was fitted to the central lumen. This change was driven by inhomogeneity of temperature measurements on the exterior of the balloon. The location of the thermocouple on the central lumen is designed to allow for a consistent temperature of the central lumen.

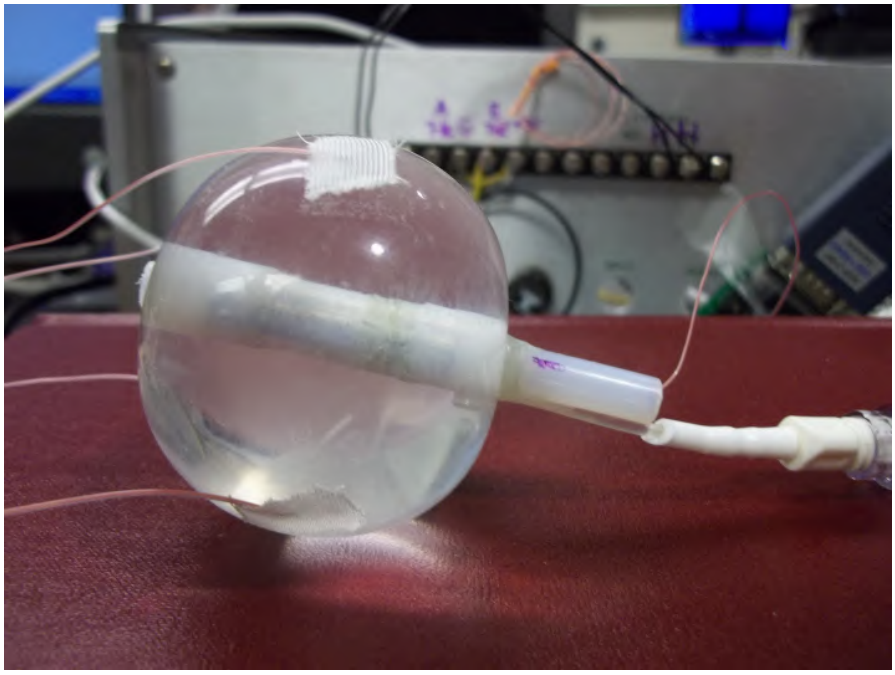

Figure 4.2 The final PBHI balloon applicator prototype.

4.2 Applicator Design Benefits/Drawbacks

The applicator design will allow for concurrent delivery of partial breast irradiation and hyperthermia nearly concurrently. The current design is very similar in dimensions to existing PBI balloon applicator designs, and is less bulky than some of the multi-lumen designs. The similarity with the construction of our applicator to current designs is a benefit. Current applicator designs have been successful in that there are very few problems encountered during the applicator placement by the physician.

Current applicators are well-tolerated by the patient population, and since our applicator is very similar, it should be similarly successful in patient comfort.

The applicator is limited to a single lumen to reduce the complexity of treatment, however multiple dwell locations can be used to somewhat shape the dose in the radial direction from the balloon lumen. The lack of multiple lumens is a somewhat moot point, however, as our applicator is design to eliminate the majority of the need for a multi-lumen design.

One potentially new issue with our applicator is the introduction of a hybrid aluminum/PTFE central lumen which will likely attenuate the radiation emitted from the central lumen more than the typical all-plastic construction that the current PBI balloon applicators use. The degree to which this is an issue will be explored further in this paper. The aluminum core may also produce increased artifact during the imaging process in x-ray, CT, and ultrasound imaging. The low density aluminum may show less artifact than if another metal had been used. Further refining of the applicator may show that the central aluminum core to the lumen may be unnecessary, if a suitable plastic replacement can be determined. This plastic would have to have to allow for a sufficient transmission of heat into the fill solution, as well as be heat resistant to the temperatures necessary for treatment.

4.3 Heating System Design

Our PBHI system requires a heating control system to deliver the hyperthermia treatment in a controlled, consistent manner. The control over how the balloon applicator

is heated is accomplished using a feedback loop system composed of miniaturized heating element that can be inserted into the balloon applicator lumen, a computerized control unit, and a thermocouple embedded into the central lumen of the balloon applicator to provide temperature information to the computerized control unit.

A thermocouple is a device used for measuring temperature. A thermocouple is a junction of two dissimilar metals that produce a voltage proportional to the temperature. Type T thermocouples were used as they have the appropriate thermal response range, come in very small sizes, and are relatively inexpensive.

The computerized control unit constantly monitors the temperature of the applicator lumen, and adjusts the output of the heating unit to raise and keep the lumen at a prescribed temperature. The manner in which the balloon is heating can be modified by adjusting parameters within the computerized control unit, as well as changing the location of the thermocouple.

4.3.1 Miniaturized Heater Design

The first aspect of the heating system that must be considered is the capability of the miniaturized heating element. The desired goals of the heating unit is that it should be able to heat the volume of fill solution within the balloon applicator to treatment temperatures within a short amount of time. The heating unit should be able to maintain a consistent temperature within the fill solution, and it should be able to maintain a homogeneous temperature within the fill solution. The miniaturized heating element that

was chosen to fill these requirements is a cylindrical, 25 mm long by 0.125 in outside diameter resistive heater (See Figure 4.3).

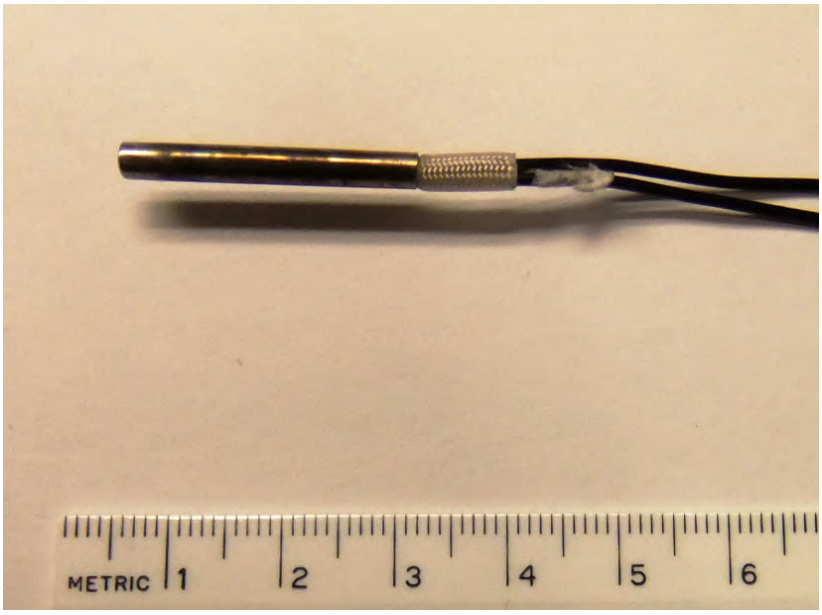

Figure 4.3 Heater used in testing of our PBHI device. A ruler is shown for scale.

A quick estimate of the heating requirements of the heater was performed to estimate the demands that would be placed on the heater. We know that we wish to heat the fill solution from body temperature (37 ^{0}C) to the our desired treatment temperature of 46 ^{0}C, and that our maximum balloon size is 6 cm in diameter (~113.1 cc). If we use the specific heat of water (4.1796 J cm^{-3} K^{-1}), and ignore the influence of convection, conduction, and heat loss, we can estimate the heat required raise our sphere to treatment temperatures (See Equation 4.1). Finding the power is simply a manner of determining how quickly this temperature is desired. To heat to 46 ^{0}C within 5 minutes would then require approximately 14 Watts, 10 minutes would require 7 Watts, etc.

$$TotalEnergy\,\mathrm{Re}\,quired = \left(4.1796\,J\,cm^{-3}K^{-1}\right)\left(9K\right)\left(113.1cc\right) = 4254.4J \qquad (4.1)$$

We purchased two heaters for testing. The first heater has a power output of 60 Watts at 24 volts with a resistance of approximately 10 Ohms at room temperature. The second heater has a power output of 2.5 Watts at 24 volts with a resistance of approximately 230 Ohms at room temperature. If we apply the previous logic, heater 1 can heat the volume of water to treatment temperature in 1.2 minutes, while heater 2 can heat the volume of water to treatment temperature in 28.4 minutes. It would seem that heater 1 is more desirable due to a speedier heating of the fill solution, however heater 2 was used in our final design for reasons that will be discussed in a later section.

4.3.2 Heat Process Controller

The miniaturized heater is controlled through the feedback loop system by the computerized control system. The basis of this system is a Watlow Series 96 proportional-integral-derivative (PID) heat process controller. The PID process controller uses the thermocouple as an input to control the heating element to arrive at a desired setpoint, which in this case will be the desired treatment temperature of the balloon fill solution. The PID can be programmed to control the manner in which the desired temperature is reached by adjusting the proportional, derivative, and integral settings. These three settings are used by the PID controller algorithm to continuously calculate a output magnitude for the heater. The PID controller calculates what the present heater output should be by first determining an error, which is simply the difference between the desired temperature and the current temperature (Astrom, 2005) (See Equation 4.2).

$$e(t) = y_{Desired} - y(t)_{Current} \qquad (4.2)$$

Where e(t) is the calculated error, $y_{Desired}$ is the set temperature, and $y(t)_{Current}$ is the measured temperature. This error, from time zero to the present, is the input for the algorithm (See Equation 4.3).

$$U(t) = K\left(e(t) + \frac{1}{T_i}\int_0^t e(\tau)d\tau + T_d \frac{de(t)}{dt} \right) \qquad (4.3)$$

The output signal U(t), which in our case is the signal controlling the heater output, is the summation of three component terms, given above in order of the proportional, integral, and derivative terms. The variable K is used to adjust the contribution of the proportional term to the final output signal, the integral time T_i is used to adjust the contribution of the integral term, and the derivative time T_d is used to adjust the contribution of the derivative term. The way in which these three components control the shape of the heating curve is not obvious. A common way to describe how each of these settings work is that the proportional setting adjusts the output based on the current error, the integral setting adjusts the output based on past error, and the derivative setting adjusts the output based on a predicted future error.

The PID settings can be tuned to arrive at the set temperature in a custom, controlled manner, and can be described as overshoot and oscillate (See Figure 4.4) The proportional setting will control how quickly the heater will respond to a difference in the current temperature and the set temperature (Astrom, 2005). Increasing the weight on the proportional component will increase how quickly the output will respond to an error between the set point and the current temperature.

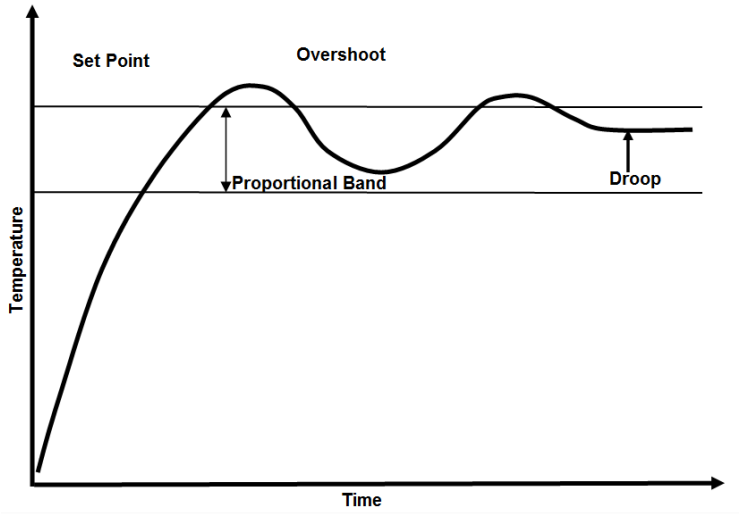

Figure 4.4 A heating curve shown for a heating system with a proportional feedback algorithm. This type of system suffers from significant oscillation about below the desired setpoint, or steady-state error. PID process controllers are able to remedy this problem (From Watlow, 1999).

Process controllers that only use proportional control in the feedback loop suffer from a problem where the temperature tends to oscillate around a lower temperature than the setpoint. This is called steady-state error, and can be also be reduced by increasing the gain on the proportional setting. However, increasing the proportional setting too much will result in a larger magnitude of oscillation.

The integral setting is mainly useful in removing the steady-state error. Equation 4.3 illustrates that as the integral time is increased, the strength of the integral component in decreased. Increasing the strength of the integral component will also result in a larger degree of oscillation

The action of the derivative component on the heating curve is similarly murky. The predictive action of the derivative component can be though of as prediction using

linear extrapolation over the derivative time T_d. The derivative component is used to slow the rate of oscillation, or in effect, dampen out the oscillation. The action of the derivative component increases with increasing derivative time to a point, then decreases when the derivative time becomes too large. The effectiveness of the derivative component stops being effective when the derivative time is greater than about 1/6th of the period of the oscillation. The period of the oscillation increases with increasing derivative time (Astrom, 2005).

The process of manually optimizing the controller settings to arrive at a proper functioning of the heating system is a non-trivial, time-consuming task. The manufacturer of the PID process controller thus provide an automatic optimization feature for the Series 96 Watlow heat controller. This feature was used to quickly optimize the heating system for our applications, and determined a proportional factor of 2.0, an integral factor of 1.8, and a derivative factor of 0.15. An example of an optimal heating curve is shown in Figure 4.5.

The Series 96 Watlow heat controller has an input for a temperature measuring device, and can be configured for several types of thermocouples or resistance temperature detectors (RTD). Our system was set to use very small (0.81 mm diameter) thermocouples. Type T thermocouples were chosen for their high sensitivity and appropriate range characteristics. The very small gauge wire provided high sensitivity and fast response.

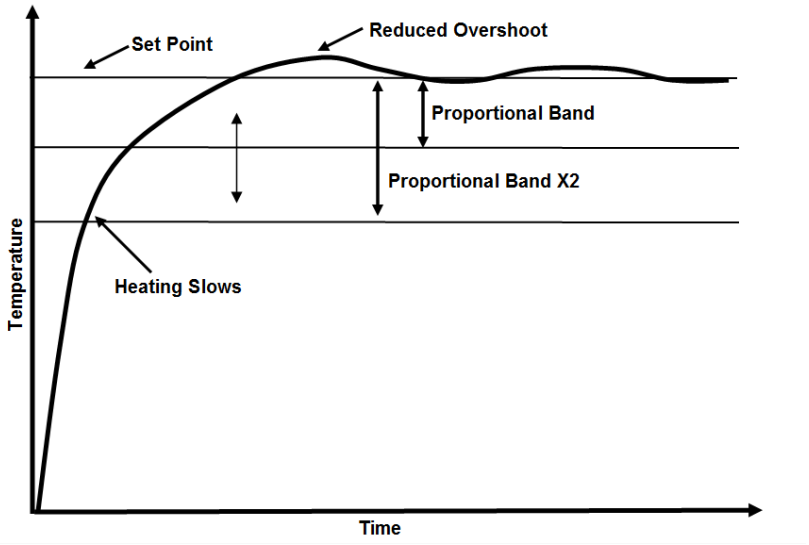

Figure 4.5 A heating curve for an optimized PID heat controller. Overshoot and oscillation are limited while arriving at the desired setpoint temperature (From Watlow, 1999).

The heat controller also has an RS-485 communications interface that was used to log heat controller data. This interface was connected to a computer through a RS-485 to USB converter to allow for connectivity with a PC. The interface required the used of termination resistors, as well as a 5 V power supply for it to work properly (Figure 4.6). Power was supplied through the use of a 24 V to 5 V voltage regulator (model LM7805). A 120 Ohm resistor was required across the transmit and receive terminals, and 1 kOhm pull up/down resistors were required from the ground and power terminals to the transmit/receive terminals to maintain the correct voltage during the idle state (Watlow, 1999).

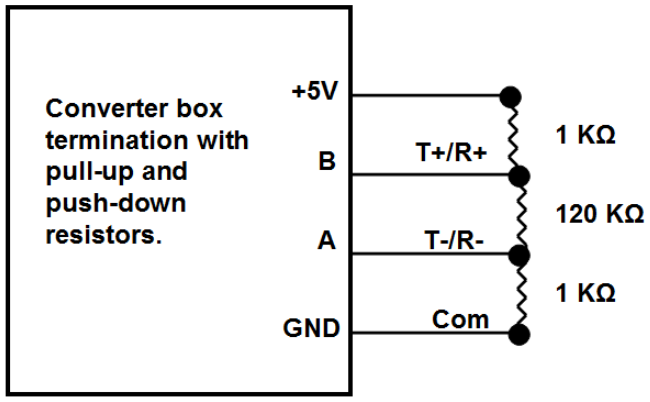

Figure 4.6 Orientation of termination and pull up/down resistors for communications interface (Adapted From Watlow, 1999).

4.3.3 Heating System Power Circuit

The Watlow Series 96 PID process controller does not supply the power for the miniaturized heater, and is only one of a handful of components that make up the heat control unit. The PID process controller runs on standard 112 V alternating-current (AC) line voltage, but uses a small (5V) direct-current (DC) signal in an on or off state to tell the heater when to turn on or off. This switching is how the PID controls the heater output, not by adjusting current to the miniaturized heating unit. This switching of the current to the heater can occur many times per second, which places significant stress upon the switching system. The most durable switch available for this type of application is a solid-state relay (SSR), which uses the small signal from the PID process controller to electronically switch the higher load of the power circuit. Since an SSR uses an electronic switch with no moving parts, it is more durable in high-demand switching environments, and faster than an electromechanical relay. The SSR used in our system is

a Carlo Gavazzi DC SSR model RD0605-D, run on a control voltage of 5 volts, and switching our power circuit voltage of 24 volts. The SSR was attached to a modified computer processor heat sink to provide heat dissipation.

The heating system requires a 24 VDC power supply to run the miniaturized heating element. The maximum current load required by the heating element was determined by V=IR. We are using a 24 VDC power supply, with a heater with 10 Ohm of resistance or a heater of 230 Ohm of resistance. The maximum current draw is therefore determined by the 10 Ohm heater to be 2.4 Amps. The power supply used is a TRC electronics RPS-60-24 power supply. This power supply provides 24 VDC output with a 66 Watts maximum power, and 2.5 Amps (~2.75 Amp max) current and runs on standard 112 VAC line voltage. The power supply is quiet and passively cooled.

The components were assembled in a reused instrument case to reduce cost (See Figure 4.7. An existing power cord socket, fuse holder, and power switch from the original equipment was retained for our system. The fuse holder is soldered between the power switch and power socket at the back of the case, and a 6 Amp fuse was installed to protect the user from shock. The ground terminal of the power socket running to the wall was attached to the case in order to ground the external box of the case. Line voltage was run from the power switch in parallel to both the 24 VDC power supply and the PID temperature controller. The circuit board of the power supply was grounded to the case to eliminate stray currents. One output from the 24 VDC power supply runs to the miniaturized heater terminal through the SSR. The second output from the power supply is converted to 5 V through the voltage regulator and powers the RS-485 communications terminal.

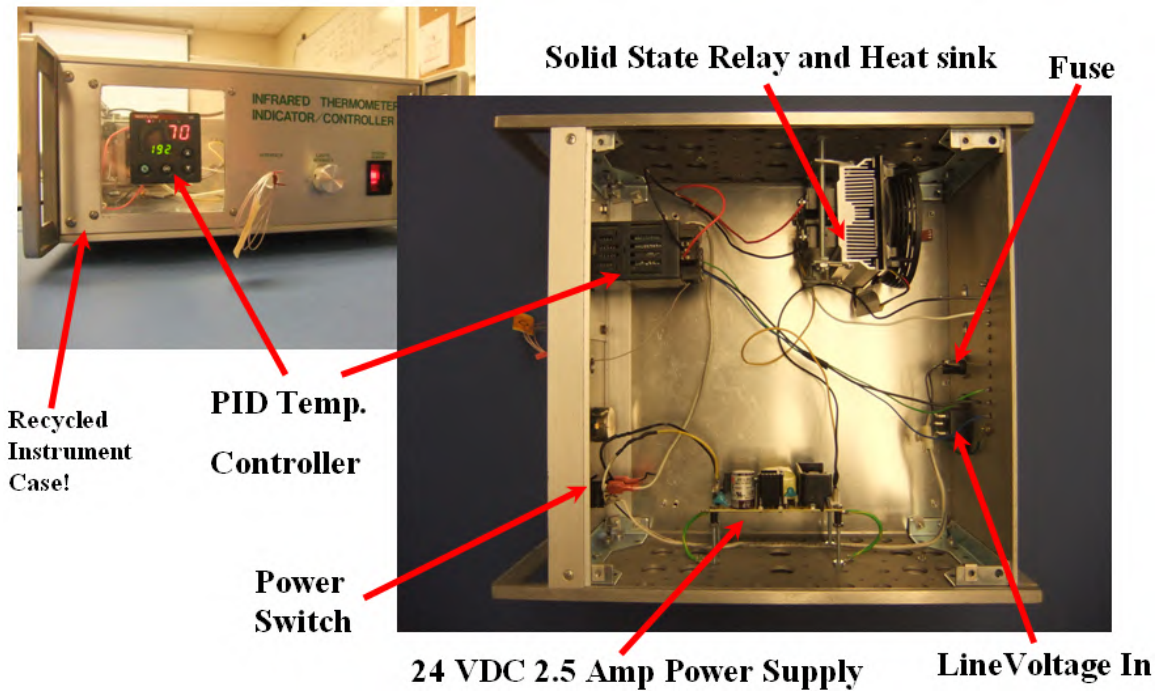

Figure 4.7 Construction of heat control unit prototype shown above. The recycled instrument case is shown with important components labeled.

4.4 Heating System Benefits/Drawbacks

The prototype heating system designed and built for our purpose is likely different from a design that may be implemented in the clinic. Our feedback-loop system is somewhat crude in that only one input temperature may be used to provide information to the PID system. In fact, a hybrid system may provide better heating management, in which several thermocouples located around the balloon, or imbedded within the patient's tissue is used to provide feedback information to the central heating unit.

The simplicity inherent in our system allows for a determination of what types of control system may work best in specific circumstances. The heating schedule specifics

will be discussed later in the text, as it applies to the thermal testing phase of this research.

4.5 Heating System Test Thermometry System

A system for measuring the temperature of the surface of the balloon at several points, as well as measuring the heat distribution within a phantom was required for the testing of the heating system described in this report. The requirements for the thermometry system are that several points can be measured simultaneously, with high accuracy, and that the temperature of these locations can be logged. There are many available products on the market to suite this purpose, however in the spirit of keeping the cost low, an inexpensive solution was found. The product used is a Phidgets 4-thermocouple USB interface device. This product allows for up to 4 thermocouples to be connected to a PC through a USB interface. The software required to log the 4 thermocouple temperatures versus time did not exist. However, sample software is provided with the source code in several programming languages. The sample software written in Visual Basic .Net was chosen as the framework for the modifications that would allow for software that would allow logging of temperature data for the 4 thermocouples, along with timing information. The sample code was written in event-style programming language. This type of code essentially only updates when a change in an input parameter is detected. Additional code was embedded to begin logging of all 4 thermocouples when a GUI interface button was pressed (See Appendix A). An input allows for a time interval to be set for data output to text files. Each line in the text file

includes the time interval from when the point logging began, the circuit board temperature, and the 4 thermocouple temperatures.

A second logging system was established with the Watlow PID controller. A PC connection was established to the PID controller using open-source industrial control Mango software. The free web-based software allows for connectivity to the PID, which was established through the use of a USB-to-RS232 adapter connected from the data port of the PID to a USB port of a pc. The software was used to monitor PID input and output in real-time, as well as log the output of the PID to the SSR, and the central lumen thermocouple temperature.

Chapter 5

Prototype Testing

5.1 Applicator Radiation Attenuation

The PBHI balloon applicator design incorporates a non-traditional, hybrid central lumen composed of PTFE and aluminum. Traditional PBI balloons are constructed solely of plastic, and since the most significant factor in brachytherapy is distance from the source, the plastic construction of traditional PBI balloons attenuates the radiation very little, and is ignored in treatment planning. Our PBHI balloon will indeed have increased attenuation, mostly due the inclusion of the aluminum insert in the central lumen. This increased attenuation must be quantified to investigate its impact on the radiative treatment delivered through the PBHI device.

5.1.1 Applicator Attenuation Estimation

The increased attenuation of the PBHI device can be estimated using the known dimensions and linear attenuation coefficients of the material used to construct the central lumen of the applicator. The attenuation follows the exponential decay model given by Equation 5.1.

$$I = I_0 e^{-ux} \qquad (5.1)$$

Where I is the intensity of the beam, I_0 is the original intensity of the beam, u is the linear attenuation coefficient of the material, and x is the thickness of the material. We can estimate the attenuation of the central lumen is for a single point source emitting perpendicular to the length of the central lumen. Radiation that passes in an oblique manner through the central lumen will travel through more of the lumen material and the attenuation will be increased. However, we only seek a first-order approximation, and we are not interested in these complexities.

The radioisotope of choice in the United States for high dose-rate brachytherapy is Iridium-192, which emits x-rays with a complex spectrum of radiation. Since a spectrum of radiation is emitted, using our simple model to determine the attenuation of the beam is in error, however using an average energy of 0.38 MeV for the energy spectrum given by Iridium-192 will give a good first approximation for the expected attenuation, as Iridium-192 emits most of its energy near the average. Linear attenuation coefficients for these materials are interpolated for an average energy of 0.38 MeV for Iridium-192 using the NIST tables (Hubbel & Seltzer, 1996).

The central portion of the lumen that the radiation will be attenuated by is comprised of 1.6 mm of aluminum and 0.50 mm of PTFE. The end regions of the lumen are comprised of 2.4 mm of PTFE. The attenuation effects of the external balloon can be ignored, as they are assumed to be very small due to the very thin nature of the balloon material, and are equivalent between our PBHI device and standard PBI balloons. The percent attenuation for these portions of the central lumen are given in Table 5.1. These estimates show that attenuation across the length of the central lumen should be relatively homogeneous, as the center of the lumen which contains the aluminum is estimated to

have only 0.2 percent more attenuation than the ends of the central lumen that is of composed of entirely PTFE.

Table 5.1 Percentage of radial attenuation estimated from linear attenuation coefficients for the average energy of Iridium-192.

	Aluminum Atten. (%)	Teflon Atten. (%)	Total Atten. (%)
Center of Lumen	4.0	1.1	5.1
Ends of Lumen	N/A	4.9	4.9

The estimated attenuation is shown to be relatively small, despite the inclusion of the aluminum/PTFE central lumen. This result is not entirely unexpected, as the most significant factor in brachytherapy is distance from the source. We can compare the expected attenuation of the PBHI applicator to the expected attenuation due to the Mammosite applicator. We do not know the composition of the plastic used in the Mammosite applicator, however if we assume it has similar properties to polyethylene, one of the most common types of plastic with appropriate physical characteristics, we find that for a 1.5 mm wall thickness, a 1.5% attenuation would result. This yields an increase in attenuation due to our applicator of only approximately 3.5%. These results suggest that potential increased attenuation due to the construction materials of the central lumen of the PBHI balloon will not be a significant problem for implementing its use to deliver radiation therapies as well as hyperthermia.

5.1.2 Applicator Attenuation Measurement

The estimate of the increased attenuation is not foolproof, as some assumptions that were made are not true to the actual conditions. These assumption include that the

radiation does not travel oblique through the central lumen, and that the spectrum of energies inherent in Iridium-192 decay is sufficiently modeled by an average energy of 0.38 MeV. In fact, the errors introduced by these assumptions are difficult to resolve in a model without using advanced techniques such as Monte Carlo simulation.

Another method for determining the additional attenuation due to the hybrid central lumen over the traditional plastic central lumen is to measure it directly. Direct measurement of the increased attenuation at all points around the central lumen requires a technique that can measure isodose distributions. The goal of our measurements is to compare the isodose distributions delivered with identical treatment plans through a standard Mammosite balloon applicator to that of our PBHI applicator to measure the potential increased attenuation. The method used in this paper is to use EBT-2 dosimetric gafchromic film. Gafchromic film is a radiosensitive sheet that darkens upon exposure to radiation. Gafchromic film has good properties as a radiation detector; it is sensitive to a wide range of doses, is insensitive to light, can measure a distribution of doses rather than a single point, and does not need to be developed such as traditional film. Several drawbacks exist for gafchromic film and these include that it requires a calibration for measuring absolute dose, and that it can be rather noisy in low-dose areas (~0-50cGy). The noise can be reduced through various analytic techniques.

Analysis of gafchromic film dosimetry was done using RIT film analysis software. The film was first digitized using a flatbed scanner which assigns each pixel a value based on the amount of light transmitted through the film, or transmittance. A calibration curve is required to convert from a transmittance value to absolute dose. Creating a calibration curve requires that a series of known doses is delivered to the

gafchromic film. A transmittance value is then found for each known dose, and a calibration curve of transmittance versus dose values can then be created which can be used to convert another exposed film from transmittance to dose.

A calibration curve was created by using the parallel method of exposing the films. The parallel method of exposing film simply means that the source dwells at the edge of the film, which results in the film being exposed to a large dose gradient, with the film nearest the source receiving a large dose, and the film farthest from the source receiving a much smaller dose to the exponential fall-off of dose inherent to brachytherapy.

Our setup consisted of using two polymethyl methacrylate (Plexi-glass) plates to sandwich the gafchromic film between. The polymethyl methacrylate served to keep the film flat, while providing a small amount of buildup, though the very low energy of radiation from Iridium-192 should require none. A transfer tube was taped to the edge of the polymethyl methacrylate and carefully centered to keep the source at the edge of the film.

A treatment plan was created using Varian BrachyVision software. The plan created delivered a dose of 800 cGy to 1 cm distance from the source. A range of distances from 5 mm to 5 cm were chosen and their corresponding doses were recorded. The gafchromic film was exposed using this treatment plan and the subsequent film was scanned using the flatbed scanner with a resolution of 160 dpi and 24 bit-color. This scanner image was then imported into RIT film analysis software using the red channel only, and opened in the parallel film calibration module. Gafchromic film is most

sensitive in the red channel, which means that the transmittance variation within the red-channel will have the larges magnitude. In the calibration module of RIT, a point was placed on the imported image at each distance doses were previously recorded for, and the transmittance value at that distance was mapped to a specific dose. An unexposed piece of film was also simultaneously scanned to provide a base transmittance value. This value was included in the calibration curve. The resulting calibration curve was saved for later use and is given in Figure 5.2. This curve shows a relatively linear response of the gafchromic film below approximately 250 cGy, with the film becoming more saturated above approximately 800 cGy. The smallest dose measured with the gafchromic film and included in the calibration curve is 32.5 cGy, which corresponds to farthest measured point on the film from the source.

Figure 5.1 A calibration curve measured for EBT-2 gafchromic film.

The magnitude of the error present within the calibration of the gafchromic film is not necessary for our application. The goal of these measurements is to compare the attenuation characteristics of a standard Mammosite balloon to our PBHI balloon by comparing the isodose distributions measured using the gafchromic film due to radiation emitted through the respective applicator lumens. Since we will be applying the same calibration curve to both films, the calibration curve accuracy is not exquisitely important, and can be further ignored. In fact, a calibration curve is unnecessary, but converts the unwieldy transmittance values into the more applicable dose units. Notwithstanding, it is estimated that the application of the calibration curve will result in dose values are accurate to within 10 percent.

The exposure of the gafchromic films for the comparison of the Mammosite and PBHI balloon attenuation was accomplished in a similar manner to the film exposure for calibration, with some variation in setup. The PBHI central lumen was used without the balloon attached to remove a source in error and complication in setup, and similarly, the balloon was removed from the Mammosite applicator that was used in the test. The polymethyl methacrylate was used to sandwich the film, however a space the size of the applicator was removed from the polymethyl methacrylate to allow for the applicator to sit within the center of the film. This technique allowed the film to be exposed radially from the applicator, measuring a dose distribution in the coronal plane. A dose of 800 cGy to 1 cm was delivered to each film for the PBHI and Mammosite applicator. A series of 4 holes were drilled through the polymethyl methacrylate at the corners to create landmarks that would be in the same place for both the PBHI and Mammosite film to allow for accurate localization between the two films in RIT. Both sets of film were

digitized using the same settings as used for the dose calibration, careful to also scan each film in the same direction and each film was cut from the same larger piece of film. Each film was imported into RIT using only the red channel. Each digitized film was converted to dose, and a template was created to align the two images to each other using the landmarks. An isodose overlay was created in RIT to compare the isodose distribution of the two films. Since the same treatment plan was used to irradiate the films for both applicators, the only difference in the isodose distribution should be due to the material composition of the applicators. The isodose overlay is shown in Figure 5.2.

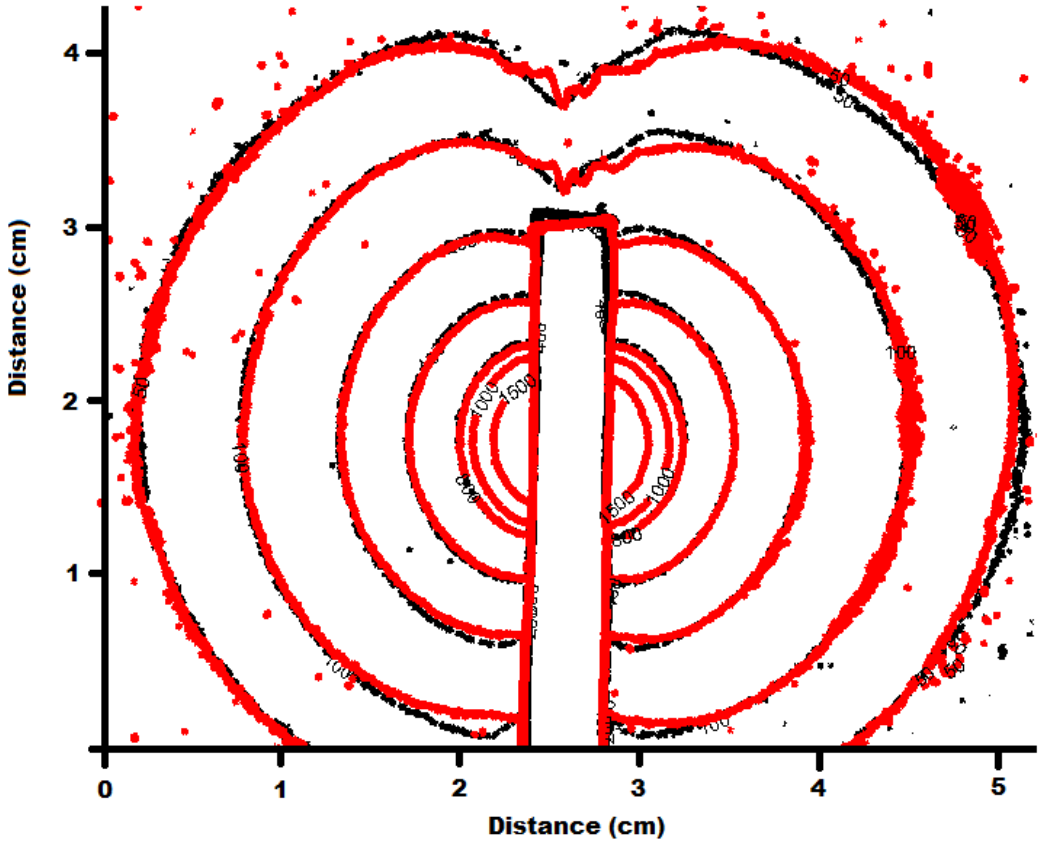

Figure 5.2 An isodose overlay for identical single dwell position treatment plans. The red isodose lines are the PBHI treatment applicator, and the black isodose lines are the Mammosite applicator.

A qualitative assessment of the isodose overlay in Figure 5.2 observes that the two isodose sets are very similar. The predicted 3.5 percent radial increased attenuation predicted by the simple approximation may be too small to observe, or may be an over-estimate. The largest difference in isodose lines appears to be in a small region near the tip of the applicators. There is noise evident on the 50 cGy isodose line, which is characteristic of gafchromic film. A technique is now available which may reduce the noise at the low-dose region of the film. This technique requires the use of a newer version of the gafchromic film, as well as the FilmQApro software, and uses the three channels of the color flat-bed scanner to correct for differences in film thickness and inconsistencies.

Additional assessment of the increased attenuation can be found by looking at dose profiles through the radial direction of the film (See Figure 5.3). One characteristic of Figure 5.3 is that the noise level of the film as illustrated by the percent difference curve in green, is quite significant, and may have a magnitude larger than the expected difference in attenuation between the applicators. As expected, this noise level appears to increase in magnitude as the dose falls to less than about 75 cGy. Another observation is that between approximately 0.5 - 1.0 cm distance from the center of the applicator, the dose for the PBHI applicator is actually greater than that of the Mammosite applicator. The magnitude of the difference is very small, and the dose gradient is very large. Due to these characteristics, this result is incredibly sensitive to errors in setup. There is also a higher dose recorded for the PBHI applicator from approximately 4 - 5 cm, which is also the low signal-to-noise region of the film. The most likely explanation for these phenomena is that the differences in attenuation are so small, that they are masked by the

error inherent in the experimental setup. Another explanation could be found in spectra changes due to the interaction of the x-ray with the material of the central lumen, however the results of the experiment are not conclusive in this regard. This type of possibility could be best answered by Monte Carlo simulation.

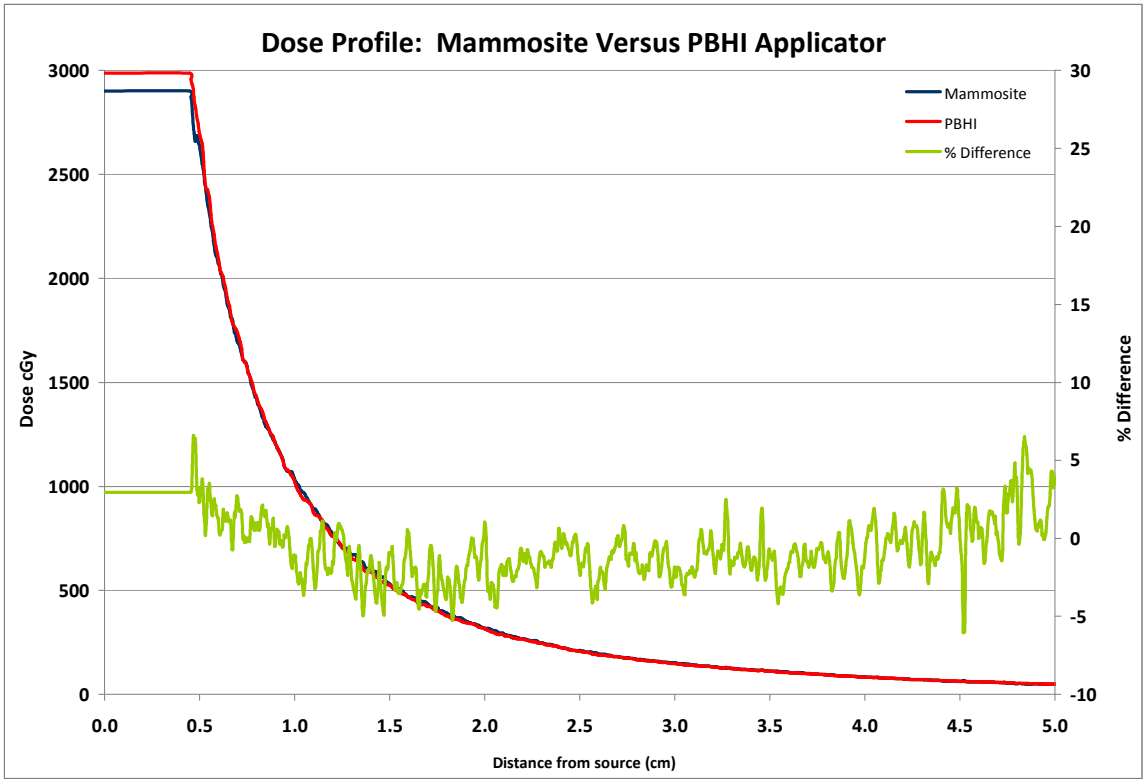

Figure 5.3 Axial dose profile for the attenuation experimental comparison of the PBHI applicator to that of a standard Mammosite applicator.

The experimental attenuation test performed for the PBHI applicator achieved the goals stated prior; to determine if the hybrid applicator significantly attenuated the radiation delivery significantly more than the standard PBI applicators on the market. The comparison to the attenuation of the Mammosite applicator shows that the increased attenuation is very small, on the order of 0-3.5 percent radially, and is within the experimental setup error of our test. The isodose distribution shown in Figure 5.2

illustrates that the isodose profiles are very similar, show an increased attenuation near the tip of the applicator, and the difference in attenuation is not likely to significantly impact treatment. New treatment planning algorithms for brachytherapy include heterogeneous corrections which may compensate for the small amount of increased attenuation due to the PBHI applicator. A refined test with more recent film and software could be performed to reduce the noise within the test performed, however this is unlikely to yield significantly improved results. The minimal impact of the hybrid applicator is expected, as the most significant variable for brachytherapy is distance from the source due to the exponential fall-off of dose with distance.

5.2 Applicator Heat Transfer

The goal of our PBHI system is to deliver hyperthermia and radiation treatments concurrently. The thermal heating properties of the balloon applicator must meet several requirements. These requirements include that the applicator temperature can be precisely controlled and can heat the tissue to hyperthermic temperatures within a clinically realistic time frame. Testing of the PBHI applicator is required to show that it is capable of meeting these requirements.

5.2.1 Thermometry System Calibration

Testing the heating properties of the PBHI balloon applicator requires the use of the previously discussed four thermocouple thermometry system. This system though accurate, requires calibration of the thermocouples to ensure that they all respond similarly when exposed to the same thermal environment. Prior to calibration, the 4

thermocouples reported a 1 degree Celsius range of temperatures around the temperature measured by the mercury thermometer.

The calibration was accomplished by exposing repeatedly all the thermocouples to a known temperature, and logging the response of the thermocouples. A hot water bath was prepared and a mercury thermometer was placed in the hot water bath. The temperature of the hot water bath was allowed to stabilize. The 4 thermocouples were repeatedly inserted into the hot water bath and removed to cycle the temperatures they should be reading (See Figure 5.4).

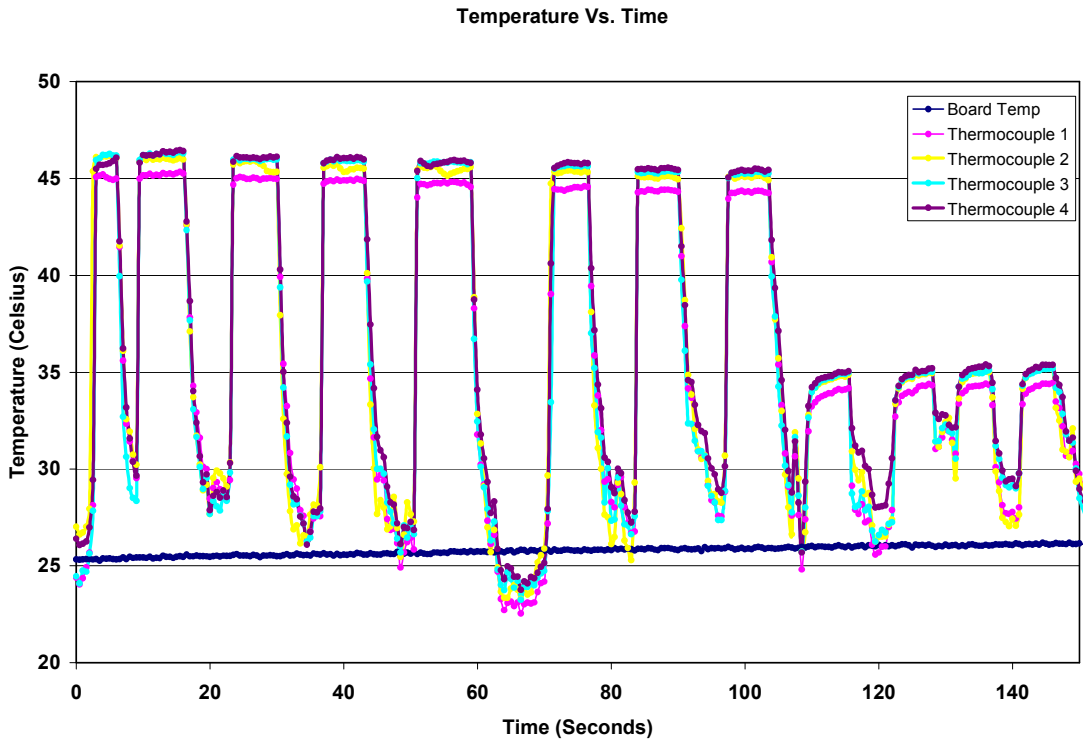

Figure 5.4 Thermocouple calibration data. Temperature was cycled to produce several data points to be averaged.

The temperature of the hot water bath was measured and recorded according to the mercury thermometer at the beginning and end of the temperature cycling. The

temperatures were logged by our thermometry system, and then imported into Microsoft Excel for plotting and analysis. The cooling trend was assumed to be linear between the beginning and ending temperature as measured by the mercury thermometer. This trendline was removed from the data for each thermocouple, which also moved their baseline to zero. The distance each thermocouple then read above or below zero was then averaged for each cycle to get a correction for each thermocouple. After calibration, each thermocouple reported the temperature within 0.5 degree Celsius of the temperature reported by the mercury thermometer and of each other.

5.2.2 Thermocouple Location

The first applicator prototype placed the thermocouple that provides feedback for the heating system at the balloon-tissue interface. This location was chosen for the thermocouple as it could provide a real-time measurement of the surface temperature of the tissue, and control the heating unit accordingly. However, initial testing showed that convection within the balloon is significant, and placing the thermocouple on the balloon surface results in large hot and cold spots within the fill solution. This problem is magnified when the thermocouple reaches the set point and the heater is cycled off, as the cold spots remain cold and are not heated to the desired temperature. The hot and cold spots are at a maximum when the thermocouple is placed at the top of the balloon, as the fluid surrounding the heated central lumen convects to the top of the balloon, when the thermocouple at the top reaches the set point, the heater turns off and the fill solution at the bottom of the balloon remains underheated.

Several solutions for this problem have been proposed; one solution is to redesign the applicator with a mixing device. One possibility is a mixing device in the form of a fan or pump. Small micro-pumps are already on the market that could be located internally to the balloon applicator, or located externally, with transfer tubes running to the balloon. Locating the device externally would allow for it to be radiation-neutral, so that it does not affect the radiation delivery. This solution may prove technically difficult, as the pump input and output would have to be located to maximize fluid mixing within the balloon applicator.

Another solution suggested by Dr. Dennis of UTMC is to use a fill solution that does not readily convect at the temperatures involved. This solution bears merit, however it would still suffer from potential long treatment times, and is analogous to the solution used by our group, since convection is driven by fluid properties as well as the temperature gradient of the fluid.

A third potential solution, that is the route followed by our group, was to change the location of the thermocouple from the balloon surface to the central lumen of the applicator. This change results in the central lumen of the balloon applicator to never rise significantly above the set point, in our case the desired temperature of the balloon fill solution. One potential drawback of this solution is that the time required to heat the balloon fill solution to treatment temperature is increased. However, the discrepancy in the temperature difference of the fill solution is reduced.

One solution to the long heating time required for the balloon applicator is to fill the balloon with solution already at the treatment temperature. This method reduces the

heating system requirements from heating up the fill solution to maintaining the temperature of the fill solution. This method could be used clinically, and would only require the balloon to be deflated and reinflated with a heated fill solution before every treatment.

5.2.3 Balloon Surface Temperature

Initial testing of the surface temperature of the balloon using the central lumen location of the thermocouple was conducted with two initial conditions. The first condition was with the fill solution at body temperature, or 37 degree Celsius. The second initial condition was with the fill solution at the desired treatment temperature, or 46 degrees Celsius. In order to isolate the balloon from external temperature fluctuations, a thermal isolation phantom was sculpted out of high-density block pouring foam. Cavities the shape and size of half of the filled PBHI applicator balloon were carved into each piece of foam. The surface of the foam cavities were coated in silicone sealant to eliminate sharp edges capable of popping the PBHI balloon. Foam is a good insulator, and is an appropriate substitute for thermally isolation over breast tissue. No measurements were made at depth in the foam, only at the surface of the balloon-foam interface.

The first phase of testing comprised of measuring how the thermal distribution on the balloon surface reacted to heating the balloon fill solution from body temperature to treatment temperature (37 ^{0}C to 46 ^{0}C), by keeping the central lumen temperature at 46 ^{0}C. First, the balloon was expanded to 6 cm diameter radially with 37 ^{0}C water, and the 4 thermocouples were placed at the top, bottom, left, and right axes of the balloon with

respect to looking into the balloon from the path of the heating element and radioactive source. The 2.5 Watt heating element was then inserted into the applicator, and the applicator was placed within the thermal isolation phantom. The previously calibrated heat control unit was connected to the heating element. The set point of the heating control unit was initially set to 37 ^{0}C, to preheat the entire system from ambient air temperature to body temperature. Preheating of the system required approximately 30 minutes. After body temperature equilibrium was reached, the heating control unit set point was set to 46 ^{0}C. Logging was started on the 4-thermcouple thermometry system, and the PID monitoring software. The heating was allowed to proceed for approximately one hour to allow the temperature of the balloon to reach treatment temperatures. The response of the thermocouples is illustrated in Figure 5.5.

A second phase of testing involved injecting treatment temperature fill solution into the balloon and recording the temperature distribution of the surface of the balloon. The exact setup used in the first phase was followed for phase two. Once body temperature thermal equilibrium was reached in the system, treatment temperature (46 ^{0}C) fill solution was injected into the balloon, and the set point of the heating control unit was set to 46 ^{0}C. The duration of the test was similar to that of the phase 1 test. The thermocouple response for this heating experiment is also reported in Figure 5.5.

The thermal testing reveals several characteristics of the heating device. Both phase 1 and 2 heating techniques result in the same endpoint thermal distribution of the surface of the balloon. When heating the fill solution from body temperature, the systems requires approximately an hour to reach a similar thermal distribution as when treatment temperature fill solution is injected into the system. Therefore, the injection of treatment

temperature fill solution can be used to drastically reduce the required treatment time duration with our system as it is currently configured.

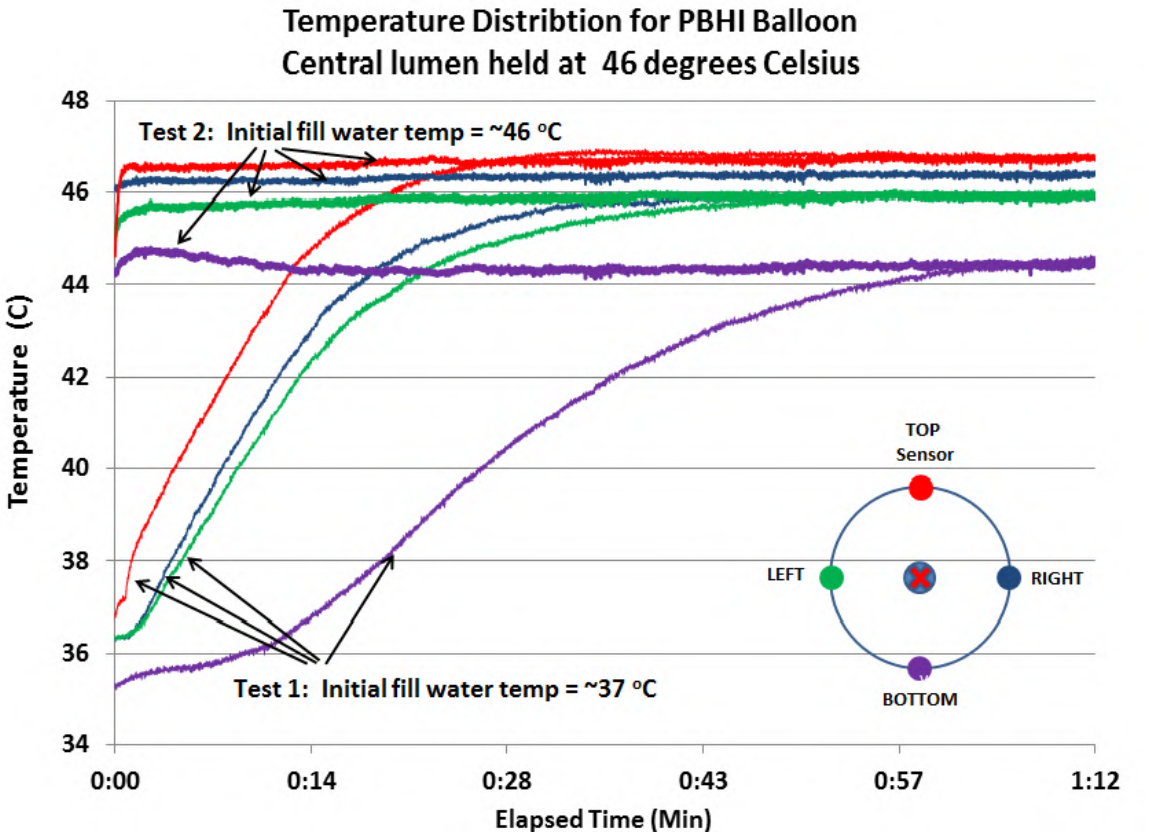

Figure 5.5 Thermal distribution of the surface of the PBHI applicator during heat testing. The central lumen temperature was held at 46 degrees Celsius for both tests.

The second aspect of the thermal distribution evident in Figure 5.5 is that inhomogeneity remains in the thermal distribution from bottom to top of the treatment balloon due to convection. The magnitude of the temperature difference is about two degrees Celsius. The left and right thermocouple also display a temperature difference that is likely due to a slight rotation of the balloon within the thermal isolation phantom. The top thermocouple reaches a temperature approximately 0.5 ^{0}C above the set point, likely due to normal cycling of the central lumen temperature about the set point.

The variation of temperature within the balloon is not ideal, and may pose complications for hyperthermia treatment with the current applicator design, as the tissue surrounding the balloon will receive variations in thermal dose. However, the difference in temperature of two degrees Celsius may be of small enough magnitude, that a sufficiently long treatment time can negate the influence of the temperature difference. The stratification of the temperature variation within the balloon is likely not to be resolved without the use of a mixing device previously described. A second benefit of a mixing device is that the temperature of the central lumen could be again controlled by a thermocouple placed on the surface of the balloon. This placement is ideal, as the central lumen temperature could be allowed to reach a much higher temperature, resulting in less time for the balloon to reach the treatment temperature. This placement normally results in significant heterogeneity in the balloon fill solution temperature, however the mixing device would quickly return the fill solution to a homogeneous temperature.

5.2.4 Porcine Tissue Heating Model

A porcine tissue heating model experiment was conducted to determine if the balloon applicator is capable of heating tissue to the treatment temperatures within a clinically realistic time frame. The porcine tissue (pork fat) was used as an analog to human breast tissue. The modeling performed established that the most significant factor affecting the heating response of tissue is the thermal conductivity of the tissue in question. Thermal conductivity of porcine fat as measured by laboratory experiments is approximately 0.2 W/mK, which is about half the thermal conductivity used for breast tissue in our modeling experiment of 0.4 W/mK. As such, the porcine tissue should

provide a conservative model for the time required to heat tissue to treatment temperatures.

The experimental setup is similar to the setup used in the phase 1 and 2 testing of the temperature distribution of the balloon surface. However, since this experiment additionally involved heating porcine tissue, it was decided that to ensure that the whole system started at a consistent temperature, the initial temperature would be room temperature. The thermal response of a system to some degree does rely on the absolute temperature of that system, however since the magnitude of the temperature difference between body temperature and room temperature is approximately 10-15 degrees Celsius, an assumption is made that the system will respond similarly at both temperatures. The system thermal response should depend mainly on the temperature difference between the balloon and the tissue. Since we wish to hold the balloon surface at 46 ^{0}C, and heat the surrounding tissue from body temperature (37 ^{0}C), we have a temperature difference of 9 ^{0}C. Room temperature during the experiment was approximately 27.5 ^{0}C, so a set point of 36.5 ^{0}C was used for the balloon fill temperature. The results were then linearly scaled so that the start temperature of the tissue was 37 ^{0}C.

The thermocouples were arranged to measure the tissue temperature, with one placed on the top of the balloon at the balloon-tissue interface. The porcine tissue consisted of a piece of fat measuring approximately 3 cm by 2 cm by 2 cm thick. Thermocouples were placed at 0, 5, 10, and 15 mm depth within the porcine tissue. The tissue was placed on top of the balloon, and the tissue was heated from room temperature to treatment temperature. The duration of the experiment was approximately an 90 minutes. The thermocouple response is shown in Figure 5.6.

The same simple model described in Chapter 3 was modified to match the parameters of the experimental setup in order to compare the results of the modeling with the experimental results. The same 3 cm radius balloon was modeled with a surrounding sphere of 5 cm radius tissue, or 2 cm tissue outside the balloon surface. The thermal parameters for the tissue were modified to better represent porcine tissue. This included changing the thermal conductivity to 0.23 W/mK, and the density to 0.930 g/cm^3.

The experimental porcine model shown in Figure 5.6 in general closely matches the computer porcine model, except for close proximity to the balloon surface. Hyperthermic temperatures (>41 ^{0}C) are reached within both the model and experimental measurements at 1 cm distance at approximately 35 minutes heating duration. The largest source of error is seen for the 0.5 cm distance temperature, closest to the time zero, and the balloon surface temperature. The discrepancy seen at the balloon surface is due to how the model works. The temperature of the balloon is held at 46 ^{0}C in the model, while the temperature measured on the balloon surface shows temperature averaging between the balloon surface and the tissue. However, since the initial temperature of the balloon in the model begins at 46 ^{0}C, the initial temperatures of the tissue close to the balloon surface are generally much higher, and this is seen in the 0.5 cm model heating curve.

Both experimental and computer models show that the heating rate slows and becomes aysmptotic as the time duration of heating increases. One difference however, is that after approximately 60 minutes the computer model shows very slow continual heating, while the experimental results show that the temperatures increase very slowly

after this point. This difference is likely due to environmental heat loss in the experimental setup.

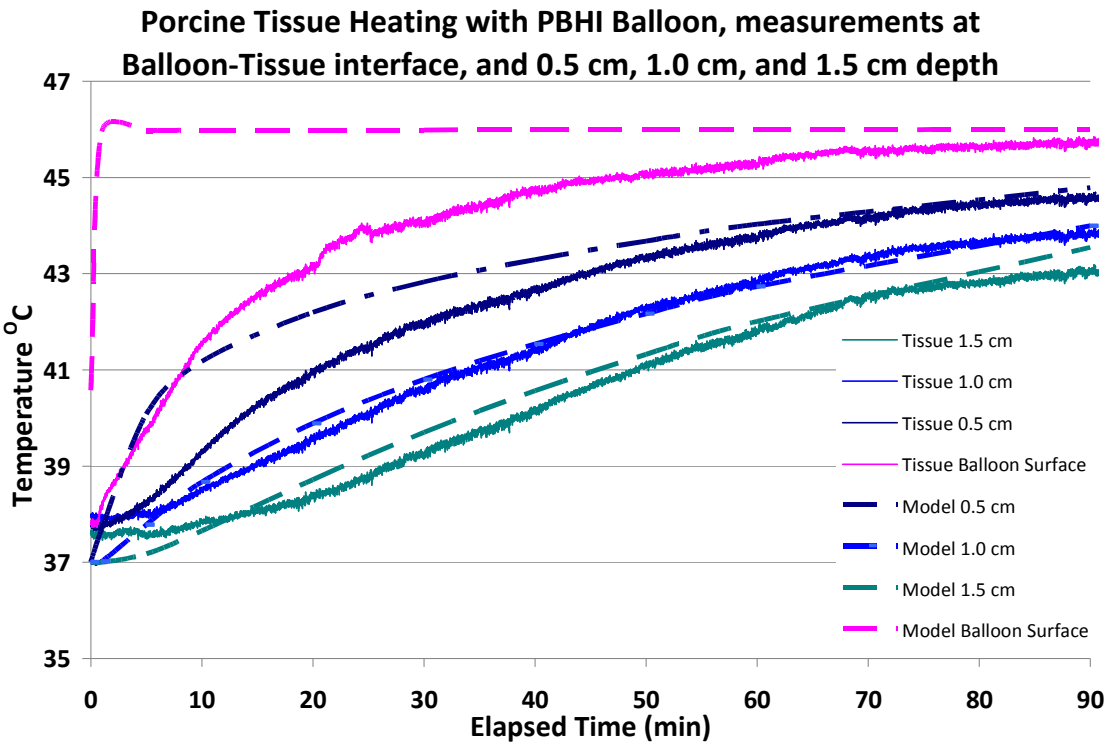

Figure 5.6 Porcine tissue heating model showing temperatures at various locations within the tissue. Shown for comparison is the model results at 1 cm for heating of breast tissue.

The good agreement between the computer porcine model and the experimental porcine model are encouraging and show that this type of treatment could potentially be effectively modeled to determine the most efficient type of thermal parameters for treatments. Another result of the modeling and experimental results showing good agreement is that it may be possible to predict breast tissue heating results accurately. If temperatures can accurately be predicted by models, there may be no need for *in situ* thermometry during a PBHI hyperthermia treatment.

Chapter 6

Conclusion

6.1 Summary of Important Findings

The PBHI system developed by our group has shown potential as an initial prototype to a clinically useful tool for delivering PBHI treatment for breast conservation therapy. The treatment system is able to deliver hyperthermia treatments with a miniature heating device, that can then be removed, allowing for the insertion of a transfer tube to allow for the introduction of the radioactive source for delivery of the radiation therapy. The entire prototype system cost less than $1,000 dollars to develop, and resulted in a prototype that can accurately deliver hyperthermia and brachytherapy treatments.

6.1.1 PBHI Balloon Applicator

The PBHI balloon applicator is very similar in size to a standard Mammosite applicator, and has been shown to have negligible increased attenuation (~3.5%). An applicator without an aluminum central lumen could very likely be developed resulting in an applicator with similar attenuation characteristics to standard Mammosite applicators. This is a result of the determination that very high temperatures are not likely needed for delivery of hyperthermia treatments, temperatures which many types of plastic are able to

withstand. The greatest problem with the PBHI applicator is the inhomogeneous temperature distribution within the applicator fill solution that will result in inhomogeneous tissue temperatures. A solution to this problem exists in the addition of a mixing device within the balloon applicator. One potential solution for a mixing device is to use miniature pumps either within the applicator, or externally with appropriate connective tubing that can increase the internal mixing within the device. This solution would also allow for a very rapid heating of the fill solution, as the central lumen temperature would not be restricted to the desired fill solution temperature as our current prototype relies on.

6.1.2 PBHI Heat Control Unit

The prototype heat control unit constructed for this investigation while simple, proved to be able to heat the PBHI balloon applicator to a set point within 0.5 degree accuracy. The control unit could be improved by increasing the number of feedback controls to allow for more thermocouples supplying information for the feedback system. This would result in a more robust, and controlled system. Another improvement over the existing system would be to use an SSR output on the PID controller to control the higher current SSR used in the control unit. The Watlow PID controller has an SSR output available that allows for very rapid switching on and off of the control circuit. This SSR output requires a separate power input, and is why it was not used in this project. However, it would be somewhat trivial to incorporate, and would increase the responsiveness of the heater to the feedback system. The responsiveness would be increased because the heater is controlled by the SSR turning it on and off. Increasing

the rate at which the SSR can switch on and off will allow for a higher power heater to be used, and will be able to limit its fluctuation (or error) about a set point.

6.1.3 Modeling Results

The modeling of the hyperthermia treatment with the finite-element modeling (FEM) program Comsol confirmed the viability of our device for delivering hyperthermia treatments in a clinically realistic time-frame, as well as provided useful insight into the tissue heating parameters. The range of values for tissue heating parameters than can occur within a breast, such as density, specific heat capacity, and thermal conductivity, are small. Of these parameters, thermal conductivity is the only parameter that can significantly very the thermal gradient produced by our modeling. The range of these parameters is not likely to significantly vary within the patient population, which should increase the likelihood that modeling of tissue heating could replace *in vivo* thermometry. However, blood flow was ignored in the modeling, which could hamper this possibility. Other factors may exist that are not considered as well, such as variations in patient homeostasis temperature, that could affect the modeling.

6.1.4 Radiation and Thermal Testing Results

The radiation attenuation test results show that the increased attenuation due to the hybrid construction of the central lumen is negligible, and is on the order of a few percent more than standard Mammosite applicators. As stated above, it may be possible to construct a PBHI applicator that does not have aluminum in the central lumen, and is

entirely composed of plastic, with similar attenuation characteristics to standard Mammosite applicators.

The thermal testing of the applicator showed that the current PBHI applicator suffers from temperature inhomogeneity within the balloon fill solution on the order of approximately 2 degrees once the temperature of the balloon has ceased to increase and reaches an equilibrium. This inhomogeneity is likely to require an internal mixing device to sufficiently mix the fill solution.

The experimental porcine tissue heating model shows agreement with the computer porcine model. This agreement showed that computer modeling can potentially be used as a tool for optimizing heating and treatment parameters for the PBHI treatment. Another result of the modeling and experimental results showing good agreement is that it may be possible to predict breast tissue heating results accurately, which may result in there being no need for *in situ* thermometry during a PBHI hyperthermia treatment.

6.1.5 Suggested PBHI Treatment Schedule

Hyperthermia treatments can suffer from thermotolerance, and as such, hyperthermia treatments cannot be given at standard radiation therapy fractionation schedules and still receive maximal benefit from the hyperthermia. We have suggested a treatment schedule to avoid thermotolerance to provide maximal benefit while still preserving the accelerated nature of the partial breast irradiation treatment. The fractionation schedule is to deliver 220 cGy twice a day, every two days, with the hyperthermia treatment being given prior to the morning fraction, and for a total of 10 fractions. We have assumed that our hyperthermia treatment will result in a TER of 1.6,

and that the tumor doubling time of breast cancer is sufficiently long that delivering the radiation treatment in two weeks is analogous to delivering it in one week.

This treatment radiation dose was used to determine a sufficient skin-to-balloon thickness for our treatment. From this we extrapolated that only 1 mm of skin is required between the balloon surface and skin to keep the skin from being overdosed. As an alternative, if the standard APBI dose of 340 cGy were used with our treatment, improved local recurrence would be the expected outcome, the increase being hard to quantify, but logically should exist.

6.1.6 Potential Alternative Delivery Method

Another type of hyperthermia delivery method, similar in the style of this paper, may also provide a solution for the inhomogeneous heating of the fill solution found in our balloon applicator. Microwaves have been used to induce tissue heating for hyperthermia, and microwave antenna may be built small enough to be introduced into the central lumen of a balloon applicator. This type of radiation allows for deeper tissue penetration than a hot-water balloon type of applicator and may provide a promising avenue for PBHI therapy.

References

Bernier, J. et. al. (2006). Partial Irradiation of the Breast: Old Challenges, New Solutions. *The Breast, 15*, 466-475.

Lehman, M. and Hickey, B. (2010). The Less Than Whole Breast Radiotherapy Approach. *The Breast*, *19*, 180-187.

Sauer, G. et. al. (2005). Partial Breast Irradiation after Breast-Conserving Surgery. *Strahlentherapie und Onkologie*, *181*, 1-8.

Njeh, C. et. al. (2010). Accelerated Partial Breast Irradiation (APBI): A Review of Available Techniques. *Radiation Oncology*, *5(90)*, 1-28.

Polgar, C. and Major, T. (2009). Current Status and Perspectives of Brachytherapy for Breast Cancer. *International Journal of Clinical Oncology, 14*, 7-24.

Detwiler, J. et. al. (2010). Dosimetric Comparison of Three Multi-Lumen Brachytherapy Applicators with the Original Mammosite Balloon Used in Partial Breast Irradiation. *2010 AAPM Spring Meeting.*

Nuclear Regulatory Commission (NRC). (2011). Reports Associated with Events. Retrieved February 1, 2011, from http://www.nrc.gov/reading-rm/doc-collections/event-status.

Van der Zee, J. (2002). Heating the Patient: A Promising Approach? *Annals of Oncology, 13*, 1173-1184.

Chichel et al. (2007). Description of a Method and a Review of Clinical Applications. *Reports of Practical Oncology and Radiotherapy, 12(5)*, 267-275.

Hall, E and Giaccia, A. (2006). *Radiobiology for the Radiologist.* 6th edition. Lippincott Williams and Wilkins Publishing, Philadelphia PA.

Jones, E. et. al. (2005). Randomized Trial of Hyperthermia and Radiation for Superficial Tumors. *Journal of Clinical Oncology, 23(13),* 3079-3085.

Horsman, M. R. and Overgaard, J. (2007). Hyperthermia: A Potent Enhancer of Radiotherapy. *Journal of Clinical Oncology, 19*, 418-426.

Vernon et. al. (2006). Radiotherapy With or Without Hyperthermia in the Treatment of Superficial Localized Breast Cancer: Results from Fiver Randomized Controlled Trials. *International Journal of Radiation Oncology Biology Physics, 35(4)*, 731-744.

Overgaard et. al. (2005). Randomised Trial of Hyperthermia as Adjuvant to Radiotherapy for Recurrent or Metastatic Malignant Melanoma. *The Lancet, 345*, 540-543.

Théberge, V. et. al. (2011). Altered Fractionization: Rationale and Justification for Whole and Partial Breast Hypofractionated Radiotherapy. *Seminars in Radiation Oncology*, 21, 55-65.

Jadwiga, W. et. al. (2007). Clinical and Dosimetric Experience with Mammosite-based Brachytherapy Under the RTOG 0413 Protocol. *Journal of Applied Clinical Medical Physics*, 8(4), 176-184.

Comsol Multiphysics. (2006). *Comsol User's Manual.* Comsol Multiphysics, Burlington, VT.

He, Y. et. al. (2006). A Numerical Coupling Model to Analyzed the Blood Flow, Temperature, and Oxygen Transport in Human Breast Tumor Under Laser Irradiation. *Computers in Biology and Medicine, 36*, 1336-1350.

Gautherie, M. (1980). Thermopathology of Breast Cancer: Measurement and Analysis of *In Vivo* Temperature and Blood Flow. *Annals of New York Academy of Sciences*, *335*, 383-415.

Astrom, K. and Hagglund, T. (2005). *Advanced PID Control*. The Instrumentation, Systems, and Automation Society. NC.

Watlow. (1999). *Watlow Series 96 User's Manual.* Watlow Controls. Winona, MN.

Hubbel, J.H. and Seltzer, S.M. (1996). Tables of X-Ray Mass Attenuation Coefficients and Mass Energy-Absorption Coefficients from 1 keV to 20 MeV for Elements Z = 1 to 92 and 48 Additional Substances of Dosimetric Interest. Retrieved January 1, 2011, from http://www.nist.gov/pml/data/xraycoef/index.cfm

Appendix

Data Logging Code For 4-Thermocouple USB Interface

The following code is a modified form of sample interface code for use with the Phidgets 4-thermocouple USB interface device. The original sample program written in Visual Basic .Net, and is copyrighted under the Creative Commons Attribution 2.5 Canada License. This copyright allows any type of use, including commercial, as long as the appropriate attribution is made. The sample software allows the user to attach to the interface device, display the temperature of one thermocouple, and allow for the thermocouple type to be selected to apply a calibration. The modified software program includes data logging capability for all four thermocouples as well as the board temperature sensor. The user is able to select a data logging interval, and is able to stop and start the logging process by selecting a GUI button. The output file is in comma-separated variable format and includes the time-stamped temperature of each of the four thermocouples and the board sensor temperature.

```
' - TemperatureSensor full -
' This is the modified example software.  The software has been modified to export temperature data in comma-seperated variable format
' for all four thermocouples.  The modified software retains the original functionality of the example software
' The example software displays the connected Phidget TemperatureSensor device's details as well as the current sensor readings
' being generated by one thermocouple, as well as demonstrates the ability to modify the sensor's sensitivity
' by setting it to a new double value in the provided textbox.
'
' Please note that the example software was designed to work with only one Phidget TemperatureSensor connected.
'
' Modified version Copyright 2011 Todd White @ University of Toledo Medical Center
' Original sample software Copyright 2007 Phidgets Inc.
' This work is licensed under the Creative Commons Attribution 2.5 Canada License.
' To view a copy of this license, visit http://creativecommons.org/licenses/by/2.5/ca/
Imports System.IO
Imports System.Timers


Public Class Form1
    Dim WithEvents phidgetTemperature As Phidgets.TemperatureSensor
    Dim sw As StreamWriter = New StreamWriter("TestFile.txt")
    Dim time As DateTime = DateTime.Now
    Dim ttest As Integer

    Public Sub New()
        ' This call is required by the Windows Form Designer.
        InitializeComponent()
        ' Add any initialization after the InitializeComponent() call.
    End Sub


    'Initialize our temperatureSensor object and hook the event handlers
    Private Sub Form1_Load(ByVal sender As System.Object, ByVal e As System.EventArgs) Handles MyBase.Load
        SensitivityTrk.SetRange(0, 200)
        SensitivityTrk.Enabled = False

        phidgetTemperature = New Phidgets.TemperatureSensor
        phidgetTemperature.open()

    End Sub
```

```
    'TemperatureSensor Attach event handler...We'll populate the fields in the GUI and
enable the modify sensitivity textbox
    Private Sub temperatureSensor_Attach(ByVal sender As Object, ByVal e As
Phidgets.Events.AttachEventArgs) Handles phidgetTemperature.Attach
        attachedTxt.Text = sender.Attached.ToString()
        nameTxt.Text = sender.Name
        serialTxt.Text = sender.SerialNumber.ToString()
        versionTxt.Text = sender.Version.ToString()
        numThermoTxt.Text = sender.thermocouples.Count.ToString()

        SensitivityTrk.Enabled = True
        SensitivityTrk.Value = phidgetTemperature.thermocouples(0).Sensitivity * 100.0
        sensitivityTxt.Text = phidgetTemperature.thermocouples(0).Sensitivity.ToString()
        'Set the ranges
        thermoRange.Text = "(" +
phidgetTemperature.thermocouples(0).TemperatureMin.ToString() + "°C to " + _
                    phidgetTemperature.thermocouples(0).TemperatureMax.ToString() +
"°C)"
        ambientRange.Text = "(" +
phidgetTemperature.ambientSensor.TemperatureMin.ToString() + "°C to " + _
                    phidgetTemperature.ambientSensor.TemperatureMax.ToString() +
"°C)"
        Try
            potentialRange.Text = "(" +
phidgetTemperature.thermocouples(0).PotentialMin.ToString() + "mV to " + _
                    phidgetTemperature.thermocouples(0).PotentialMax.ToString() +
"mV)"
        Catch ex As Phidgets.PhidgetException
            'really old temperature sensors do not support this
            If ex.Type =
Phidgets.PhidgetException.ErrorType.PHIDGET_ERR_UNSUPPORTED Then
                potentialRange.Text = "(Not Supported)"
            End If

        End Try

            thermoTypeComboBox.Enabled = True
            Select Case phidgetTemperature.thermocouples(0).Type
                Case
Phidgets.TemperatureSensorSensor.ThermocoupleType.PHIDGET_TEMPERATURE_S
ENSOR_K_TYPE
                    thermoTypeComboBox.SelectedItem = "K-Type"
                Case
Phidgets.TemperatureSensorSensor.ThermocoupleType.PHIDGET_TEMPERATURE_S
ENSOR_J_TYPE
                    thermoTypeComboBox.SelectedItem = "J-Type"
```

```
            Case
Phidgets.TemperatureSensorSensor.ThermocoupleType.PHIDGET_TEMPERATURE_S
ENSOR_E_TYPE
                thermoTypeComboBox.SelectedItem = "E-Type"
            Case
Phidgets.TemperatureSensorSensor.ThermocoupleType.PHIDGET_TEMPERATURE_S
ENSOR_T_TYPE
                thermoTypeComboBox.SelectedItem = "T-Type"
        End Select

        Select Case phidgetTemperature.thermocouples(1).Type
            Case
Phidgets.TemperatureSensorSensor.ThermocoupleType.PHIDGET_TEMPERATURE_S
ENSOR_K_TYPE
                thermoTypeComboBox.SelectedItem = "K-Type"
            Case
Phidgets.TemperatureSensorSensor.ThermocoupleType.PHIDGET_TEMPERATURE_S
ENSOR_J_TYPE
                thermoTypeComboBox.SelectedItem = "J-Type"
            Case
Phidgets.TemperatureSensorSensor.ThermocoupleType.PHIDGET_TEMPERATURE_S
ENSOR_E_TYPE
                thermoTypeComboBox.SelectedItem = "E-Type"
            Case
Phidgets.TemperatureSensorSensor.ThermocoupleType.PHIDGET_TEMPERATURE_S
ENSOR_T_TYPE
                thermoTypeComboBox.SelectedItem = "T-Type"
        End Select

    End Sub

    'TemperatureSensor Detach event handler....Clear the fields and disable the modify
sensitivity textbox so that
    'new sensity value can't be sent while there is no device attached, otherwise this would
generate a PhidgetException
    Private Sub temperatureSensor_Detach(ByVal sender As Object, ByVal e As
Phidgets.Events.DetachEventArgs) Handles phidgetTemperature.Detach
        attachedTxt.Text = sender.Attached.ToString()
        nameTxt.Text = ""
        serialTxt.Text = ""
        versionTxt.Text = ""
        numThermoTxt.Text = ""
        thermoTempTxt.Text = ""
        onboardTempTxt.Text = ""
        SensitivityTrk.Enabled = False
        SensitivityTrk.Value = 0
```

```
        sensitivityTxt.Clear()

    End Sub

    'Error event handler..We'll simply display the error description in a popup messagebox
window
    Private Sub temperatureSensor_Error(ByVal sender As Object, ByVal e As
Phidgets.Events.ErrorEventArgs) Handles phidgetTemperature.Error
        MessageBox.Show(e.Description)
    End Sub

    'Temperature Change event handler...We'll display the current temperature reading
from the sensor to the
    'specified textbox as they come in
    Private Sub temperatureSensor_TemperatureChange(ByVal sender As Object, ByVal e
As Phidgets.Events.TemperatureChangeEventArgs) Handles
phidgetTemperature.TemperatureChange
        If e.Index = 0 Then
            onboardTempTxt.Text =
phidgetTemperature.ambientSensor.Temperature.ToString()
            thermoTempTxt.Text = e.Temperature.ToString()
            thermoPotTxt.Text = e.Potential.ToString()
        End If
    End Sub

    'When a new double valu is entered into the textbox, we will update the sensitivity
value in the sensor
    'If no temperature sensor is attached when we try to update the sensitivity value, it will
throw a PhidgetException,
    'so we will catch it and deal with it accordingly
    'Also, the sensitivity is a double value, so we should prevent and other values to be
sent.  Since I am using the
    'Double.parse method, it will throw a FormatException if anything other than a double
value is entered, so
    'we'll catch that and deal with it accordingly


    'When the application is terminating, close the Phidget.
    Private Sub Form1_FormClosing(ByVal sender As Object, ByVal e As
System.Windows.Forms.FormClosingEventArgs) Handles Me.FormClosing

        RemoveHandler phidgetTemperature.Attach, AddressOf temperatureSensor_Attach
        RemoveHandler phidgetTemperature.Detach, AddressOf temperatureSensor_Detach
        RemoveHandler phidgetTemperature.Error, AddressOf temperatureSensor_Error
        RemoveHandler phidgetTemperature.TemperatureChange, AddressOf
temperatureSensor_TemperatureChange
```

```
        Application.DoEvents()

        phidgetTemperature.close()
    End Sub

    Private Sub SensitivityTrk_Scroll(ByVal sender As Object, ByVal e As
System.EventArgs) Handles SensitivityTrk.Scroll

        Try
            phidgetTemperature.thermocouples(0).Sensitivity = SensitivityTrk.Value / 100.0
            phidgetTemperature.thermocouples(1).Sensitivity = SensitivityTrk.Value / 100.0
            sensitivityTxt.Text = (SensitivityTrk.Value / 100.0).ToString()
        Catch ex As Exception
            sensitivityTxt.Clear()
        End Try

    End Sub
    Private Sub thermoTypeComboBox_SelectedIndexChanged1(ByVal sender As Object,
ByVal e As System.EventArgs) Handles thermoTypeComboBox.SelectedIndexChanged

        Try
            Select Case thermoTypeComboBox.SelectedItem.ToString()
                Case "K-Type"
                    phidgetTemperature.thermocouples(0).Type =
Phidgets.TemperatureSensorSensor.ThermocoupleType.PHIDGET_TEMPERATURE_S
ENSOR_K_TYPE

                Case "J-Type"
                    phidgetTemperature.thermocouples(0).Type =
Phidgets.TemperatureSensorSensor.ThermocoupleType.PHIDGET_TEMPERATURE_S
ENSOR_J_TYPE
                Case "E-Type"
                    phidgetTemperature.thermocouples(0).Type =
Phidgets.TemperatureSensorSensor.ThermocoupleType.PHIDGET_TEMPERATURE_S
ENSOR_E_TYPE
                Case "T-Type"
                    phidgetTemperature.thermocouples(0).Type =
Phidgets.TemperatureSensorSensor.ThermocoupleType.PHIDGET_TEMPERATURE_S
ENSOR_T_TYPE
                    phidgetTemperature.thermocouples(1).Type =
Phidgets.TemperatureSensorSensor.ThermocoupleType.PHIDGET_TEMPERATURE_S
ENSOR_T_TYPE
            End Select
            thermoRange.Text = "(" +
phidgetTemperature.thermocouples(0).TemperatureMin.ToString() + "°C to " + _
                phidgetTemperature.thermocouples(0).TemperatureMax.ToString() + "°C)"
```

```
        Catch ex As Phidgets.PhidgetException
            If ex.Type =
Phidgets.PhidgetException.ErrorType.PHIDGET_ERR_UNSUPPORTED Then
                thermoTypeComboBox.Enabled = False
            End If
        End Try
    End Sub

    Private Sub groupBox1_Enter(ByVal sender As System.Object, ByVal e As
System.EventArgs) Handles groupBox1.Enter

    End Sub

    Private Sub attachedTxt_TextChanged(ByVal sender As System.Object, ByVal e As
System.EventArgs) Handles attachedTxt.TextChanged

    End Sub

    Private Sub nameTxt_TextChanged(ByVal sender As System.Object, ByVal e As
System.EventArgs) Handles nameTxt.TextChanged

    End Sub

    Private Sub serialTxt_TextChanged(ByVal sender As System.Object, ByVal e As
System.EventArgs) Handles serialTxt.TextChanged

    End Sub

    Private Sub Form_Load()
        Timer1.Enabled = False
    End Sub

    'Modify interface to include timer button
    Private Sub Button1_Click(ByVal sender As System.Object, ByVal e As
System.EventArgs) Handles Button1.Click
        ttest = 0
        Timer1.Interval = TextBox3.Text
        Timer1.Enabled = True
        AddHandler Timer1.Tick, AddressOf timer1_Tick
        MessageBox.Show("Check this shit out!" & vbNewLine &
phidgetTemperature.thermocouples(0).Temperature.ToString())
    End Sub

    'Export data to file with time stamp
```

```
    Private Sub timer1_Tick(ByVal sender As System.Object, ByVal e As
System.EventArgs)
        If ttest = 0 Then
            TextBox1.Text = "Logging Started"
            sw.Write(String.Format("{0:hh:mm:ss.fff}", Now))
            sw.Write(", ")
            sw.Write(phidgetTemperature.ambientSensor.Temperature.ToString())
            sw.Write(", ")
            sw.Write(phidgetTemperature.thermocouples(0).Temperature.ToString())
            sw.Write(", ")
            sw.Write(phidgetTemperature.thermocouples(1).Temperature.ToString())
            sw.Write(", ")
            sw.Write(phidgetTemperature.thermocouples(2).Temperature.ToString())
            sw.Write(", ")
            sw.Write(phidgetTemperature.thermocouples(3).Temperature.ToString())
            sw.WriteLine()
        Else
            TextBox1.Text = "Logging Stopped"
            sw.Close()
        End If

    End Sub

    Private Sub Button2_Click(ByVal sender As System.Object, ByVal e As
System.EventArgs) Handles Button2.Click
        ttest = 1
    End Sub



End Class
```